Molecular and Functional Evaluation of Antidiabetic Activity of *Rotula aquatica* Based Silver Nanoparticles in Cellular Models

Dissertation submitted to the University of Kerala in partial fulfilment of the requirements for the award of the Degree of

MASTER OF SCIENCE IN BIOCHEMISTRY

Submitted by

SARA SIRAJ

Candidate Code: 63824142010

Exam Code: 63822403

Subject Code: BC 544

Under the Guidance of

Dr. Nadiya F. & Dr. Ansil P.N. (TKMCAS)

Inter University-Centre for Genomics & Gene Technology (IU-CGGT)
University of Kerala, Kariavattom, Thiruvananthapuram



DEPARTMENT OF BIOCHEMISTRY
T.K.M. COLLEGE OF ARTS AND SCIENCE, KARICODE, KOLLAM

JULY, 2026

Department of Biochemistry
T.K.M. College of Arts and Science
(Affiliated to University of Kerala)
Re-accredited by NAAC with "A++" Grade
Kollam – 6G1005, Kerala.
www.tkmcas.ac.in

CERTIFICATE

This is to certify that the dissertation entitled **'Molecular and Functional Evaluation of Antidiabetic Activity of *Rotula Aquatica* Based Silver Nanoparticles in Cellular Models'** submitted to the University of Kerala in partial fulfilment of the requirements for the award of the degree of Master of Science in Biochemistry, is a record of original research work carried out by **SARA SIRAJ (Candidate Code: 63824142010)** of the Department of Biochemistry, T.K.M. College of Arts and Science, Kollam under the guidance and supervision of **Dr. Nadiya F. and Dr. Ansil P.N.,** in the Inter University Centre for Genomics and Gene Technology (IU-CGGT), University of Kerala, Kariavattom. It is also certified that no part of this work has been presented for the award of any other degree, diploma, or similar title at any other university.

Dr. Ansil P. N.
Internal Guide

Dr. Ajinza A.
Head of the Department of Biochemistry

Examiners:

1.

2.

Declaration

I hereby declare that the thesis titled **"Molecular and Functional Evaluation of Antidiabetic Activity of *Rotula Aquatica* based Silver Nanoparticles in Cellular Models"** is based on original research work carried out by me under the supervision of **Dr. Nadiya F. and Dr. Ansil P.N.,** in the Inter University Centre for Genomics and Gene Technology (IUCGGT), University of Kerala. I further declare that no part of this work has been presented for the award of any other degree, diploma, or similar title from any other university.

SARA SIRAJ

Acknowledgements

The successful completion of this dissertation is due to the guidance, encouragement, and support of many individuals. I would like to express my heartfelt gratitude to the Almighty for blessing me with good health, strength, wisdom, and perseverance throughout my postgraduate studies and in completing this research work.

I sincerely thank **Prof. (Dr.) R. Rajalakshmi**, Hon. Director, Inter University Centre for Genomics and Gene Technology (IUCGGT), for granting me the opportunity and providing the facilities required to carry out this research at the centre.

I owe my deepest gratitude to my research guide, **Dr. Nadiya F**., Research Associate, IUCGGT, whose constant guidance, expert suggestions, patience, and encouragement inspired me throughout this study. Her support and valuable insights have been invaluable in the successful completion of this dissertation.

I especially thank my beloved principal, **Prof. Dr. M. J. Sheeba,** T.K.M. College of Arts and Science, Karicode, Kollam, for providing me with such a wonderful platform to complete my project.

I am extremely thankful to **Dr. Ajinza A**., Head of the Department of Biochemistry and my internal guide **Dr. Ansil P. N.,** other faculty members **Dr. Soumya S., Dr. Sumayya A.S.** and **Dr. Hari Sankar H.S.,** for the critical guidance and encouragement.

It would be beyond words if I try to express my thanks to **Dr. Lekshmi N**, Research Associate, **Ms. Arya C.S**, and **Mr. Sajith S. K**, JRFS, IUCGGT, **Ms. Mihina B.T** who were most welcoming, cooperative and helpful throughout the course of my work.

I wish to pay my gratitude to my loving parents and friends for their constant encouragement and moral support given throughout my study period.

SARA SIRAJ

List of Contents

Chapter	Title	Page No.
	List of figures	
	List of tables	
	Abbreviations	
	Abstract	
1	Introduction	1 – 9
2	Review of Literature	10 - 18
3	Aim and Objectives	19
4	Materials and Methods	20 – 32
5	Results	33 – 46
6	Discussion	47 – 50
	Summary and Conclusion	51
	Reference	52 - 61

List of Figures

Figure No.	Title	Page No.
1	a) *Rotula aquatica* plant and b) Root sample collected for the study	6
2	Stages of silver nanoparticle synthesis from root extract	33
3	UV–Visible absorption spectrum of RQR-AgNPs	34
4	FTIR spectrum of RQR-AgNPs	35
5	Size range of RQR silver nanoparticles obtained by DLS analysis	36
6	Dose-dependent effect of *Rotula aquatica*-mediated silver nanoparticles on HepG2 cell viability	37
7	Graph showing cell viability against various concentrations of *Rotula aquatica*-mediated silver nanoparticles (HepG2 cells)	38
8	Dose-dependent effect of *Rotula aquatica*-mediated silver nanoparticles on L6 cell viability	39
9	Graph showing cell viability against various concentrations of *Rotula aquatica*-mediated silver nanoparticles (L6 cells)	40
10	Alpha-amylase inhibition by *Rotula aquatica*-mediated silver nanoparticles	41
11	Standard curve of 2-deoxyglucose-6-phosphate (2-DG6P)	42
12	Dose-response curve showing stimulation of 2-deoxyglucose uptake by *Rotula aquatica* extract	43
13	Agarose gel electrophoresis of total RNA isolated from samples	44
14	Representative qRT-PCR amplification and melt curve analysis of the GAPDH reference gene used for cDNA quality assessment	45
15	Relative expression of the GLUT4 gene in treated and control samples determined by qRT-PCR	46

List of Tables

Table	Title	Page No.
1	Taxonomic classification of *Rotula aquatica*	6
2	Dose-Dependent reduction in HepG2 cell viability	36
3	Showing the cell viability of *Rotula aquatica* mediated silver nanoparticles against each concentration of the drug in HepG2 cells	37
4	Cytotoxicity evaluation of doxorubicin and *Rotula aquatica* mediated silver nanoparticles in HepG2 based on IC_{50} value.	38
5	Dose-Dependent reduction in L6 cell viability	38
6	Showing cell viability of *Rotula aquatica* mediated silver nanoparticle against each concentration of the drug in L6 cells	40
7	Cytotoxicity evaluation of doxorubicin and *Rotula aquatica* mediated silver nanoparticles in L6 based on IC_{50} value	40
8	Alpha amylase inhibition by *Rotula aquatica* mediated silver nanoparticle against standard	41
9	OD reading of 2-DG6P standards	42
10	Concentration -dependent effect of *Rotula aquatica* extract on 2-DG uptake	43

Abbreviations

AgNPs : Silver nanoparticles

BSA : Bovine serum albumin

cDNA : Complementary DNA

CDC : Centers for Disease Control and Prevention

Ct : Cycle threshold

DEPC : Diethyl pyrocarbonate

DM : Diabetes mellitus

DMEM : Dulbecco's Modified Eagle Medium

DMSO : Dimethyl sulfoxide

DPP-IV : Dipeptidyl peptidase IV

DPPH : 2,2-Diphenyl-1-picrylhydrazyl radical

DNSA : 3,5-Dinitrosalicylic acid

DTNB : 5,5′-Dithiobis-(2-nitrobenzoic acid)

DLS : Dynamic Light Scattering

2-DG6P : 2-Deoxyglucose-6-phosphate

EFRA : Ethyl acetate fraction of *Rotula aquatica*

FBS : Fetal bovine serum

FTIR : Fourier-transform infrared spectroscopy

IC_{50} : Half maximal inhibitory concentration

IDDM : Insulin-dependent diabetes mellitus

IDF : International Diabetes Federation

MTT : 3-(4,5-Dimethylthiazol-2-yl)-2,5-diphenyltetrazolium bromide

PBS : Phosphate-buffered saline

PPAR-γ : Peroxisome proliferator-activated receptor gamma

PTP1B : Protein tyrosine phosphatase 1B

qRT-PCR: Quantitative Real-Time Polymerase Chain Reaction

RNA : Ribonucleic acid

RQR : *Rotula aquatica* root extract

RQR-AgNPs : *Rotula aquatica* root extract-mediated silver nanoparticles

SEM : Scanning electron microscopy

SPR : Surface plasmon resonance

UV–Visible : Ultraviolet–Visible spectrophotometry

WHO : World Health Organization

Abstract

The increasing prevalence of type 2 diabetes mellitus has created a need for safer and more effective therapeutic agents. Green synthesis of silver nanoparticles using medicinal plants has emerged as an eco-friendly and cost-effective approach due to the biological activities of plant-derived phytochemicals. *Rotula aquatica*, an important medicinal plant, possesses several pharmacological properties; however, its potential in nanoparticle-mediated antidiabetic therapy remains largely unexplored.

The present study aimed to synthesize silver nanoparticles using *Rotula aquatica* root extract and evaluate their physicochemical characteristics and antidiabetic potential. The synthesized nanoparticles were characterized by UV–Visible spectroscopy, Dynamic Light Scattering (DLS), and Fourier Transform Infrared (FTIR) spectroscopy. Their biological activities were assessed using MTT cytotoxicity assay in HepG2 and L6 cell lines, α-amylase inhibition assay, glucose uptake assay in L6 cells, and quantitative real-time PCR (qRT-PCR) analysis of *Glut-4* gene expression.

UV–Visible spectroscopy confirmed the formation of silver nanoparticles with a characteristic surface plasmon resonance peak at 447 nm. DLS analysis revealed a uniform particle size of approximately 45–50 nm with good colloidal stability, while FTIR analysis confirmed the involvement of phytochemicals in nanoparticle synthesis and stabilization. The MTT assay demonstrated concentration-dependent cytotoxicity, with lower toxicity observed in L6 skeletal muscle cells than in HepG2 cells. The synthesized nanoparticles exhibited significant α-amylase inhibitory activity (73.2%), comparable to the standard drug metformin. Glucose uptake in L6 cells increased in a concentration-dependent manner, with the highest uptake observed at 100 µg/mL. Furthermore, qRT-PCR analysis demonstrated significant upregulation of *Glut-4* mRNA expression in nanoparticle-treated L6 cells, suggesting enhanced insulin-mediated glucose transport.

The findings of this study indicate that *Rotula aquatica*-mediated silver nanoparticles possess promising antidiabetic activity through α-amylase inhibition, enhanced cellular glucose uptake, and increased *Glut-4* gene expression. These results suggest that the synthesized nanoparticles may serve as a potential plant-based nanotherapeutic candidate for the management of type 2 diabetes mellitus. However, further in vivo studies and molecular investigations are required to confirm their therapeutic efficacy and safety.

Chapter 1

Introduction

Diabetes mellitus (DM) is one of the most prevalent endocrine disorders worldwide, affecting millions of people and posing a major public health challenge. It comprises a group of metabolic disorders characterised by chronic hyperglycaemia resulting from defects in insulin secretion, insulin action, or both. Elevated blood glucose levels lead to the classic symptoms of diabetes, including polyuria (frequent urination), polydipsia (excessive thirst), and polyphagia (increased hunger) (Ismail et al., 2009). As a persistent metabolic disorder, diabetes mellitus has become an escalating global health concern with significant social, medical, and economic consequences. According to global estimates, approximately 285 million adults aged 20–79 years were living with diabetes in 2010, representing 6.6% of the world's adult population. This number is projected to increase to 438 million by 2030, accounting for 7.8% of the global adult population. India has one of the largest populations of individuals with diabetes and has often been referred to as the “diabetes capital of the world” because of its high disease burden (Joshi et al., 2007). According to the International Diabetes Federation (IDF) Diabetes Atlas 2006, the number of people with diabetes in India was estimated at approximately 40.9 million and projected to rise to 69.9 million by 2025 if effective preventive measures were not implemented.

The term “Asian Indian phenotype” refers to a distinct set of clinical and biochemical characteristics observed among Indians, including increased insulin resistance, greater abdominal adiposity, a larger waist circumference despite a relatively lower body mass index, reduced adiponectin levels, and elevated high-sensitivity C-reactive protein levels. The increasing prevalence of diabetes mellitus in India has been largely attributed to changing dietary patterns, sedentary lifestyles, and reduced physical activity, particularly in urban populations (Ramachandran et al., 2010). Consequently, diabetes has emerged as a major public health concern in India, affecting more than 62 million diagnosed individuals. In 2000, India had the highest number of individuals with diabetes mellitus, estimated at 31.7 million, followed by China with 20.8 million and the United States with 17.7 million. The global prevalence of diabetes was projected to increase dramatically from 171 million cases in 2000 to 366 million cases by 2030, with India expected to experience the largest increase. It was estimated that by 2030, approximately 79.4 million people in India would be affected by diabetes mellitus, while the numbers in China and the United States would rise to 42.3 million and 30.3 million, respectively (Wild et al., 2004; Whiting et al., 2011). Diabetes mellitus is

broadly classified into two major types: insulin-dependent diabetes mellitus (IDDM or Type I diabetes) and non-insulin-dependent diabetes mellitus (NIDDM or Type II diabetes). Type 1 diabetes is an autoimmune disorder characterised by inflammation and destruction of pancreatic β-cells within the islets of Langerhans, leading to an absolute insulin deficiency. In contrast, Type II diabetes is characterised by insulin resistance and impaired insulin secretion, leading to chronic hyperglycemia (Arora et al., 2009). The presence of diabetes mellitus significantly increases the risk of several complications, including cardiovascular disease, peripheral vascular disorders, stroke, neuropathy, nephropathy, retinopathy, blindness, and limb amputation. Pharmacological interventions are primarily employed to control blood glucose levels, alleviate symptoms, prevent long-term complications, and improve the quality of life of diabetic patients. Insulin replacement therapy remains the cornerstone of treatment for individuals with Type I diabetes, whereas dietary modifications, lifestyle changes, and oral hypoglycemic agents play a crucial role in the management of Type II diabetes (Bastaki et al., 2005). Various classes of antidiabetic drugs, including insulin, biguanides, and sulfonylureas, are commonly used to manage diabetes. However, their use is often associated with several adverse effects that may limit long-term compliance and therapeutic efficacy (Eshrat et al., 2003).

Insulin is a peptide hormone produced by the β-cells of the islets of Langerhans in the pancreas and is widely used in the treatment of diabetes mellitus. Common adverse effects associated with insulin therapy include hypoglycemia, allergic reactions, lipodystrophy, edema, and weight gain. Metformin, a member of the biguanide class, is one of the most commonly prescribed oral antidiabetic drugs. It primarily acts by reducing hepatic glucose production and improving insulin sensitivity. Reported side effects of metformin include lactic acidosis, cholestatic hepatitis, and vitamin B12 deficiency (Asplund et al., 2008). Glibenclamide is an oral hypoglycemic drug belonging to the sulfonylurea class and functions by stimulating insulin secretion from pancreatic β-cells. Common side effects include Hypoglycemia, allergic reactions, blurred vision, gastrointestinal disturbances, and intrahepatic cholestasis. Glimepiride, another sulfonylurea with intermediate to long-acting properties, lowers blood glucose levels by enhancing insulin release from pancreatic β-cells. Adverse effects associated with glimepiride include Hypoglycemia, allergic reactions, weight gain, Cholecystitis, and gastrointestinal symptoms such as nausea, vomiting, heartburn, anorexia, and diarrhea (Bhatia et al., 1970).

Medicinal plants and their bioactive constituents have gained considerable attention as alternative or complementary therapeutic agents for the management of diabetes mellitus, particularly in regions where access to conventional medicines is limited. These plants contain a wide range of phytochemicals with significant therapeutic potential. Although several synthetic drugs are available for diabetes management, their use is often associated with high costs and undesirable side effects. Consequently, herbal medicines have emerged as attractive alternatives owing to their affordability, accessibility, and comparatively lower incidence of adverse effects (Jacob et al., 2019). According to the World Health Organisation (WHO), nearly 90% of people in developing countries depend on medicinal plants and plant-derived products for their primary healthcare needs. The WHO has documented approximately 21,000 plant species used for medicinal purposes worldwide, of which nearly 2,500 species occur in India. Among these, about 800 plant species have been reported to possess antidiabetic properties. Numerous plant-derived bioactive compounds have demonstrated promising therapeutic potential for the prevention and management of diabetes mellitus (Patel et al., 2012).

Several medicinal plants native to India have been traditionally used to manage diabetes mellitus. Some of the most widely studied and therapeutically important species include babul (*Acacia arabica*), bael (*Aegle marmelos*), agrimony (*Agrimonia eupatoria*), onion (*Allium cepa*), garlic (*Allium sativum*), ghrita kumara (*Aloe vera*), neem (*Azadirachta indica*), ash gourd (*Benincasa hispida*), beetroot (*Beta vulgaris*), fever nut (*Caesalpinia bonducella*), bitter apple (*Citrullus colocynthis*), ivy gourd (*Coccinia indica*), eucalyptus (*Eucalyptus globulus*), banyan tree (*Ficus benghalensis*), gurmar (*Gymnema sylvestre*), gurhal (*Hibiscus rosa-sinensis*), sweet potato (*Ipomoea batatas*), purging nut (*Jatropha curcas*), mango (*Mangifera indica*), bitter gourd (*Momordica charantia*), mulberry (*Morus alba*), kiwach (*Mucuna pruriens*), tulsi (*Ocimum sanctum*), bisasar (*Pterocarpus marsupium*), pomegranate (*Punica granatum*), jamun (*Syzygium cumini*), giloy (*Tinospora cordifolia*), and fenugreek (*Trigonella foenum-graecum*). These plants are rich sources of phytochemicals, including alkaloids, flavonoids, phenolic compounds, tannins, terpenoids, and glycosides, which contribute to their antidiabetic properties. *Ficus religiosa*, commonly known as peepal, belongs to the family Moraceae and has been extensively used in Ayurvedic medicine for the management of diabetes mellitus (Simmonds & Howes, 2006). Various studies have demonstrated that *F. religiosa* exhibits a wide range of pharmacological activities, including hypoglycemic, hypolipidemic, anticonvulsant, anti-inflammatory, analgesic, antimicrobial, antiviral, antioxidant, antitumor, antiulcer, anxiolytic, anthelmintic, antiasthmatic, immunomodulatory, estrogenic, endothelin

receptor-blocking, apoptotic, nootropic, and antihypertensive effects (Singh et al., 2011). In traditional medicine, a decoction prepared from its bark is commonly used to treat diabetes. The plant contains several bioactive compounds, including tannins, saponins, polyphenols, flavonoids, and sterols, which are believed to contribute to its therapeutic potential.

Momordica charantia, commonly known as bitter gourd or karela, belongs to the family Cucurbitaceae. The fruit and seeds of this plant are widely utilised for their medicinal properties. Bitter gourd has been traditionally used in Asia, South America, and East Africa for the treatment of diabetes and cardiovascular disorders. In addition to its medicinal value, it is commonly consumed as a vegetable. The fruit contains several bioactive compounds, including charantin, vicine, triterpenoids, and various antioxidants, which contribute to its antidiabetic effects (Krawinkel et al., 2006). Numerous preclinical studies have demonstrated the hypoglycemic and antidiabetic activities of *M. charantia* through multiple mechanisms of action (Leung et al., 2009). Furthermore, the plant has been reported to possess antibacterial, antiviral, anticancer, and antidiabetic properties, although most investigations have focused on its role in diabetes management (Basch et al., 2003; Grover & yadav, 2004). Several animal studies have shown that bitter gourd can improve metabolic syndrome, a condition in which diabetes is a major risk factor (Gadang et al., 2011; Shih et al., 2009; Wang et al., 2011). In addition, a clinical study conducted in Taiwanese adults reported significant reductions in waist circumference along with improvements in diabetic status and metabolic syndrome-related parameters following bitter gourd consumption (Tsai et al., 2012).

Ocimum sanctum L., commonly known as holy basil or tulsi, belongs to the family Lamiaceae. Various parts of the plant have been traditionally used to treat numerous ailments. Tulsi is widely distributed throughout tropical and subtropical regions and is valued for its nutritional and medicinal properties. Eugenol, one of the major bioactive constituents of *O. sanctum*, is considered primarily responsible for many of its therapeutic effects (Pattanayak et al., 2010). The leaves and stems of *O. sanctum* contain a diverse range of bioactive compounds, including flavonoids, saponins, tannins, triterpenoids, rosmarinic acid, apigenin, isothymusin, isothymonin, cirsimaritin, orientin, and vicenin. The essential oil extracted from tulsi leaves contains eugenol, ursolic acid, carvacrol, linalool, limatrol, and caryophyllene. The seeds contain fatty acids and sitosterol, while the seed mucilage is rich in carbohydrates. The green leaves are also a source of anthocyanins. In addition, tulsi is rich in vitamins, minerals, chlorophyll, and various phytonutrients that contribute to its medicinal value.

The antidiabetic properties of tulsi have long been recognised in Ayurveda (Khan et al., 2012). Studies have reported significant reductions in blood glucose, glycosylated haemoglobin, and urea levels, along with marked increases in glycogen, haemoglobin, and total protein levels in streptozotocin-induced diabetic rats treated with ethanolic extracts of *O. sanctum* (Narendhirakannan et al., 2006). Furthermore, leaf extracts of *O. sanctum* have been shown to enhance insulin secretion pathways (Hannan et al., 2006). A 30-day treatment with *O. sanctum* extract in normal rats resulted in a significant reduction in serum glucose levels (Nair et al., 2005). Additionally, *O. sanctum* has been reported to decrease cortisol and glucose levels in male mice, suggesting potent antioxidant and antiperoxidative activities. Among the medicinal plants used in traditional healthcare systems, *Rotula aquatica* Lour. occupies a prominent position in Ayurveda and other indigenous systems of medicine. *R. aquatica* is a small, aromatic, highly branched shrub belonging to the family Boraginaceae. It commonly grows in flowing freshwater ecosystems and on-stream banks throughout India and has considerable ecological and medicinal significance. The plant is known by several vernacular names, including Pashanbheda, Seppunerinji, and Kallurvanchi. It is distributed across India, Sri Lanka, tropical Southeast Asia, and parts of Latin America.

Phytochemical investigations have revealed numerous bioactive constituents in *R. aquatica*, including baurenol, steroids, alkaloids, rhabdiol, allantoin, flavonoids, and phenolic compounds. These secondary metabolites are believed to contribute to the plant's therapeutic properties. Traditionally, *R. aquatica* has been used for the treatment of diabetes, hemorrhoids, sexually transmitted infections, cancer, kidney stones, bladder stones, uterine disorders, ulcers, skin diseases, and urinary tract ailments (Vysak et al., 2016).

Several pharmacological studies have demonstrated the medicinal potential of *R. aquatica*, including antimitotic (Patil et al., 2004), antiurolithiatic (Venkatachalam et al., 2013), antioxidant (Pallavi et al., 2016), anti-inflammatory (Mengi & Bakshi, 2009), and anthelmintic activities (Lakshmi et al., 2012). Morphologically, *R. aquatica* is a compact, aromatic shrub that grows to a height of approximately 60–180 cm. The leaves are simple, sessile, oval-shaped, and approximately 1.5 cm long, with rounded apices and dense pubescence on both surfaces. The roots are cylindrical and typically arise from lateral branches. The flowers are small (approximately 6 mm in diameter), pink to reddish in color, and occur either singly or in clusters, possessing five stamens. The fruits are fleshy, orange-red drupes measuring about 4 mm in diameter and contain four seeds (Baby et al., 2017).



(a) *Rotula aquatica* plant (b) *Rotula aquatica* root (current study material)

Figure 1: a) *Rotula aquatica* plant and b) Root sample collected for the study

Table 1: Taxonomic classification of *Rotula aquatica* (Bency et al; 2017b)

Taxonomic rank	Classification
Kingdom	Plantae
Division	Magnoliophyta
Class	Magnoliopsida
Order	Lamiales
Family	Boraginaceae
Genus	Rotula
Species	*R.aquatica*

Rotula aquatica typically grows among stones and gravel in streambeds and is widely distributed throughout India. It commonly inhabits low-lying plains with flowing water and open, stony riverbeds, although wild populations have also been reported in tropical forest ecosystems. The species is distributed from the Kumaun region in the north to Assam in the east and extends throughout western and southern India. In India, *R. aquatica* has been reported from several states, including Kerala (Idukki, Kannur, Kasaragod, Kollam, Kottayam, Malappuram, Palakkad, Pathanamthitta, and Thrissur), Tamil Nadu (Coimbatore, Dharmapuri, Nilgiris, and Tirunelveli), Karnataka (Chikmagalur, Hassan, Mysore, Uttara Kannada, Shivamogga, and Dakshina Kannada), and Maharashtra (Nashik, Pune, Raigad, Ratnagiri, Satara, and Sindhudurg). The species is also distributed in Sri Lanka, Southeast Asia, and parts of Latin America (Vysak et al., 2016).

The root and leaf extracts of *R. aquatica* exhibit considerable antioxidant activity, with root extracts demonstrating stronger activity than leaf extracts. Among the solvent extracts tested, methanolic extracts showed the highest antioxidant potential, as assessed by various free-radical scavenging assays. These findings suggest that *R. aquatica* may have therapeutic value in the prevention and management of diseases associated with oxidative stress (Pallavi et al., 2016). Extracts of *R. aquatica* have also been reported to possess significant antimitotic activity. The tannin-rich fraction exhibited greater antimitotic effects than the non-tannin fraction. This activity was inhibited by folic acid in a dose-dependent manner, suggesting a possible mechanism of action and potential application in cancer therapy. Furthermore, the extract significantly inhibited the growth of human pancreatic cancer cell lines, highlighting its potential as an anticancer agent (Patil et al., 2004).

Studies have demonstrated that *R. aquatica* extracts can influence the crystallisation of calcium oxalate, a major component of kidney stones, by reducing crystal size in vitro. These findings indicate its potential role in the prevention and management of urolithiasis. Among the tested extracts, the aqueous root extract showed the greatest antiurolithiatic activity by promoting the formation of smaller, less damaging calcium oxalate crystals (Venkatachalam et al., 2013). The aqueous root extract of *R. aquatica* has demonstrated significant anti-inflammatory activity in various experimental rat models, including carrageenan-induced paw edema, cotton pellet-induced granuloma, and crystal-induced inflammation. Treatment with the extract resulted in a significant reduction in paw edema, decreased neutrophil and monocyte counts in inflammatory exudates, and reduced granuloma formation in a dose-dependent manner. In addition, the extract significantly lowered interleukin-6 (IL-6) levels in crystal-induced inflammatory exudates. These findings suggest its potential utility in the treatment of inflammatory disorders, particularly crystal-induced arthropathies. The extract also exhibited antioxidant properties that may contribute to its anti-inflammatory effects (Mengi & Bakshi, 2009). Furthermore, methanolic leaf extracts of *R. aquatica* have been reported to exhibit stronger anti-inflammatory activity than aqueous extracts, further supporting its therapeutic potential (Agrawal et al., 2021).

The methanolic bark extract of *R. aquatica* demonstrated dose-dependent anthelmintic activity against the adult Indian earthworm *Pheretima posthuma*. The extract induced paralysis and death of the worms, suggesting its potential application as a natural anthelmintic agent (Lakshmi et al., 2012). In addition, aqueous root extracts have shown broad-spectrum antibacterial activity against Gram-positive and Gram-negative bacteria, indicating significant

antimicrobial potential (Baby et al., 2017). Collectively, these findings highlight the diverse pharmacological properties of *R. aquatica* and support its traditional use in indigenous systems of medicine. The plant has long been utilised by rural communities for the management of diabetes mellitus and is included as an ingredient in several polyherbal formulations reported to possess antidiabetic activity (Shyam et al., 2013).

The alcoholic extract of *Rotula aquatica* has demonstrated significant antidiarrheal activity in various experimental models, including castor oil-induced diarrhoea, the charcoal meal test, and prostaglandin E_2 (PGE_2)-induced diarrhoea. The extract, administered at doses of 100 and 200 mg/kg, effectively inhibited PGE_2-induced diarrhea, possibly through the suppression of prostaglandin synthesis. The antidiarrheal effect of the extract may be attributed to its ability to reduce intestinal motility, alleviate intestinal spasms, and decrease fluid accumulation within the gastrointestinal tract, thereby providing relief from diarrheal symptoms (Baby et al., 2017).

The green synthesis of nanoparticles using plant extracts has emerged as an environmentally friendly, cost-effective, and sustainable approach to nanoparticle production. Compared with conventional physical and chemical synthesis methods, green synthesis offers several advantages, including eco-friendliness, higher product yields, reduced processing time, simpler synthesis procedures, and the use of less toxic, inexpensive solvents (Sivakumar, 2021). Furthermore, this approach requires lower energy consumption and can be carried out under mild reaction conditions. Studies have suggested that plant-mediated silver nanoparticles exhibit enhanced biological and physiological activities compared with nanoparticles synthesised through conventional chemical methods (Castillo-Henriquez et al., 2020). Silver nanoparticles (AgNPs) can be synthesised using a wide variety of plant materials. During synthesis, phytochemicals in plant extracts act as reducing agents, converting silver ions (Ag^+) into metallic silver nanoparticles (Ag^0) (Rana et al., 2020). These phytochemicals donate electrons to silver ions, facilitating their reduction and the formation of silver nanoparticles (Ahmad et al., 2019). In addition, plant-derived compounds function as stabilising and capping agents, preventing nanoparticle aggregation and oxidation (Restrepo et al., 2021). By coating the nanoparticle surface, these biomolecules enhance nanoparticle stability, dispersibility, and biocompatibility. The synergistic combination of bioactive plant constituents and metal nanoparticles underpins phytonanotherapy, a promising therapeutic approach with potential applications comparable to those of conventional synthetic drugs (Dewanjee et al., 2020).

Silver has been utilised in medicinal applications for centuries because of its remarkable antimicrobial and therapeutic properties (Medici et al., 2015). One important strategy for diabetes management involves inhibiting the carbohydrate-hydrolysing enzymes α-amylase and α-glucosidase, which play key roles in glucose metabolism. Inhibition of these enzymes delays the breakdown of complex carbohydrates into absorbable monosaccharides, thereby reducing postprandial blood glucose levels. Consequently, α-amylase inhibitors can be administered alongside carbohydrate-rich meals to minimise sudden increases in blood glucose concentrations. Several in vitro and in vivo studies have demonstrated that silver nanoparticles exhibit inhibitory activity against α-amylase and may therefore contribute to glycemic control.

Various in vitro assays are employed to evaluate the antidiabetic potential of natural products and nanomaterials. These include enzyme inhibition assays involving α-amylase, α-glucosidase, sucrase, protein tyrosine phosphatase 1B (PTP1B), and dipeptidyl peptidase IV (DPP-IV) (Jijith et al., 2017). Non-enzymatic assays include glucose uptake studies, glycated haemoglobin (HbA1c) estimation, cultured cell-line experiments, MTT-based cytotoxicity assays, and glucose transport studies using peroxisome proliferator-activated receptor gamma (PPAR-γ) luciferase reporter systems. In vivo antidiabetic evaluations have been conducted using several model organisms, including silkworms, zebrafish, rats, and mice (Hasan et al., 2018). Green-synthesised silver nanoparticles have a wide range of applications, including environmental remediation, wastewater treatment, food preservation, nano-insecticide development, nano pesticide production, and cosmetic formulations (Huq et al., 2022). Owing to their diverse biological activities, these nanoparticles are increasingly being investigated as potential therapeutic agents for diabetes management (Dinparvar et al., 2020).

Despite the availability of several antidiabetic drugs, there remains a growing demand for safer, more effective, and affordable therapeutic alternatives due to the increasing global prevalence of diabetes mellitus and the limitations associated with current treatment options. Medicinal plants have attracted considerable attention due to their diverse bioactive compounds with proven antidiabetic potential. More recently, the green synthesis of silver nanoparticles using plant extracts has emerged as a promising area of research because of its environmentally sustainable nature and broad biological applications. However, only a limited number of studies have investigated the use of *Rotula aquatica* for the synthesis of silver nanoparticles and the evaluation of their antidiabetic properties. Therefore, the present study aims to investigate the *in vitro* antidiabetic potential of silver nanoparticles synthesised using *Rotula aquatica* root extract.

Chapter 2

Review of Literature

Diabetes mellitus (DM), commonly referred to as diabetes, is a chronic metabolic disorder characterized by persistent hyperglycemia resulting from defects in insulin secretion, insulin action, or both (Farwa et al., 2022). The disease develops through complex interactions between genetic predisposition and environmental factors, leading to disturbances in carbohydrate, lipid, and protein metabolism (Galicia-Garcia et al., 2020). According to the Centers for Disease Control and Prevention (CDC), diabetes is one of the leading chronic diseases affecting diverse populations and remains a major contributor to morbidity and mortality in the United States (Gregg et al., 2014). Globally, the prevalence of diabetes has increased at an alarming rate over recent decades, making it a significant public health challenge (Sivaprasad et al., 2012). In 2019, diabetes was responsible for approximately 409,000 deaths among adults aged 20 years and older in the Americas, ranking among the leading causes of mortality in the region (Cousin et al., 2022). Diabetes substantially increases the risk of developing cardiovascular diseases, stroke, chronic kidney disease, diabetic foot ulcers, neuropathy, retinopathy, and vision impairment. Diabetes mellitus is broadly classified into Type 1 diabetes (T1D) and Type 2 diabetes (T2D). Type 1 diabetes is an autoimmune disorder characterised by the destruction of pancreatic β-cells, leading to an absolute insulin deficiency. In contrast, Type 2 diabetes, the more prevalent form, is characterised by insulin resistance accompanied by progressive β-cell dysfunction, leading to impaired glucose homeostasis (Blair, 2016).

The increasing prevalence of Type 2 diabetes has been strongly associated with sedentary lifestyles, physical inactivity, obesity, and excessive weight gain. The global prevalence of diabetes among adults increased from 4.7% in 1980 to 8.8% in 2017 and is projected to reach 9.9% by 2045, according to estimates from the International Diabetes Federation (Cho et al., 2018). In the Southeast Asian region, the number of individuals living with diabetes is expected to increase substantially, from approximately 82 million in 2017 to 151 million by 2045. Consequently, there has been growing interest in the use of medicinal plants for diabetes management, particularly within traditional systems of medicine in India and other parts of the world. Several of these medicinal plants have been scientifically evaluated for their antidiabetic properties.

The World Health Organisation (WHO) has acknowledged the importance of traditional herbal medicines in healthcare and has encouraged scientific investigation of medicinal plants for the management of chronic diseases, including diabetes mellitus (Sarkhail et al., 2007). Various classes of antidiabetic drugs, such as insulin, biguanides, and sulfonylureas, are currently used to manage diabetes. However, their long-term use is often associated with adverse effects. Insulin therapy and sulfonylureas may cause hypoglycemia and weight gain, whereas metformin has been associated with gastrointestinal disturbances, vitamin B12 deficiency, and, in rare cases, lactic acidosis. Furthermore, treatment cost, accessibility, and route of administration are important considerations in diabetes management (Haq et al., 2021). Bioactive metabolites derived from medicinal plants have attracted considerable attention because of their hypoglycemic potential and comparatively lower incidence of adverse effects (Hussain et al., 2016). In recent years, research has increasingly focused on metal nanoparticles for a wide range of biomedical applications, including biosensors, diagnostic tools, drug delivery systems, and therapeutic agents. These advances have opened new avenues for the development of nanoparticle-based strategies for diabetes management and other chronic diseases.

Medicinal plants have played a vital role in human civilisation for centuries, serving as sources of food, medicine, shelter, and livestock feed. Their importance in healthcare has been recognised since ancient times, particularly because of their rich content of bioactive phytochemicals with diverse therapeutic properties (Mamedov et al., 2012). Numerous medicinal plants have been traditionally used for the prevention and treatment of various diseases, including diabetes mellitus, and many have subsequently been scientifically validated for their antidiabetic activities (Anand et al., 2017). These findings have facilitated the development of plant-based antidiabetic therapies that are considered relatively safe, cost-effective, and easily accessible, and that are associated with fewer adverse effects than many synthetic drugs (Fitipaldi et al., 2018; Hasan et al., 2018). According to Welihinda et al. (1982), Ayurveda and other traditional systems of medicine describe a wide range of medicinal plants used to manage diabetes mellitus. These herbal remedies continue to play an important role in complementary and alternative medicine due to their affordability, accessibility, and relatively low side-effect profile. Several studies have suggested that bioactive compounds in medicinal plants may promote pancreatic β-cell regeneration, stimulate insulin secretion, enhance insulin sensitivity, and reduce insulin resistance, thereby improving glycemic control.

A large number of medicinal plants have been investigated for their antidiabetic potential and have demonstrated significant effects on glucose metabolism through diverse pharmacological mechanisms. *Achillea santolina* L. (Asteraceae) has been reported to exhibit hypoglycemic and antioxidant activities, suggesting its potential to reduce oxidative stress associated with hyperglycemia (Yazdanparast et al., 2007). Similarly, *Artemisia pallens* has been shown to lower blood glucose levels by enhancing glucose uptake in peripheral tissues (Subramoniam et al., 1996), while *Areca catechu* L. has demonstrated promising hypoglycemic effects (Chempakam et al., 1993). *Beta vulgaris* L. has been reported to improve glucose tolerance, indicating a beneficial role in postprandial glucose regulation (Yoshikawa et al., 1996). Likewise, *Boerhaavia diffusa* L. exhibits multifaceted antidiabetic activity by reducing blood glucose levels, increasing plasma insulin concentrations, and providing antioxidant protection (Pari et al., 2004). *Bombax ceiba* L. has also demonstrated significant hypoglycemic activity (Saleem et al., 1999). Furthermore, *Butea monosperma* (Lam.) and *Carum carvi* L. have been reported to possess substantial antihyperglycemic properties (Eddouks et al., 2004; Somani et al., 2006). *Cogniauxia podolaena* Baill. exhibits both hypoglycemic and antihyperglycemic activities, suggesting its involvement in glucose homeostasis through multiple mechanisms (Diatewa et al., 2004). Similarly, *Commelina communis* L. has been associated with improved glycemic control and may offer therapeutic benefits in non-insulin-dependent diabetes mellitus (Youn et al., 2004).

Curcuma longa L. has demonstrated potent hypoglycemic effects and has been shown to improve insulin sensitivity by modulating the peroxisome proliferator-activated receptor gamma (PPAR-γ) signalling pathway (Kuroda et al., 2005). *Cynodon dactylon* Pers. has also been reported to possess significant antihyperglycemic activity (Jarald et al., 2008). In addition, *Enicostemma littorale* Blume exhibits strong antidiabetic properties by reducing blood glucose levels, glycated haemoglobin concentrations, and hepatic glucose-6-phosphatase activity, thereby improving carbohydrate metabolism (Vijayvargia et al., 2000). Collectively, these studies highlight the immense potential of medicinal plants as valuable sources of bioactive compounds for the prevention and management of diabetes mellitus. Their ability to target multiple pathological mechanisms involved in diabetes makes them promising candidates for the development of novel antidiabetic therapeutics. *Rotula aquatica* Lour. has attracted considerable attention because of its diverse pharmacological properties, including antiurolithiatic, diuretic, antioxidant, anti-inflammatory, and antidiabetic activities. Owing to these therapeutic attributes, *R. aquatica* occupies an important place in Ayurvedic medicine.

This small aquatic shrub is indigenous to the Indian subcontinent and is commonly found along the rocky riverbanks of the Western Ghats. Traditionally, it has been used to treat kidney stones, urinary tract disorders, diabetes, and several other ailments (Ameena Ansar & Ansil, 2025). According to Bency et al. (2017b), *R. aquatica* is a small, highly branched shrub that grows to a height of approximately 60–180 cm. The leaves are simple, sessile, and vary from ovate to oblong in shape, with rounded apices and an average length of about 1.5 cm. The branches are densely covered with trichomes, which are also present on both leaf surfaces. The flowers are small (4–6 mm in diameter), occurring singly or in clusters, and are pink to scarlet. Each flower possesses five stamens and a short pedicel. The fruits are fleshy, orange-red drupes measuring approximately 4 mm in diameter and typically contain four seeds. Cylindrical roots frequently arise from the lateral branches of the plant.

Extensive phytochemical investigations have revealed a wide range of secondary metabolites in *R. aquatica*, including alkaloids, flavonoids, phenolic compounds, saponins, terpenoids, steroids, tannins, amino acids, and proteins (Pallavi et al., 2016; Sasikala et al., 2013). Pallavi et al. (2016) reported that methanolic root extracts exhibited the highest total phenolic content, while both methanolic and chloroform extracts of roots and leaves contained substantial quantities of flavonoids and phenolic compounds. These phytochemicals contribute significantly to the plant's medicinal value due to their potent antioxidant and health-promoting properties. The antioxidant potential of *R. aquatica* has been demonstrated through several in vitro studies involving root and leaf extracts. The plant exhibits strong free-radical scavenging activity against DPPH, nitric oxide, hydroxyl, and superoxide radicals. In addition, it possesses metal-chelating activity and inhibits lipid peroxidation, thereby protecting cells from oxidative damage (Aswathanarayan & Vittal, 2013; Pallavi et al., 2016; Vijayakumari et al., 2013). Both enzymatic and non-enzymatic antioxidant assays have indicated that the roots contain the highest concentration of antioxidant constituents.

Several studies have documented the pharmacological activities of *R. aquatica*, particularly its antiurolithiatic effects. Investigations by Christina et al. (2002), Raut et al. (2008), and Sasikala et al. (2013) demonstrated that root extracts inhibit calcium oxalate crystal formation and promote the dissolution of urinary calculi in both in vitro and in vivo models. Furthermore, studies conducted by Ancy et al. (2018) and Vysakh et al. (2022) reported significant nephroprotective activity of ethyl acetate and methanolic extracts of *R. aquatica*. These extracts were found to attenuate gentamicin-induced nephrotoxicity and pyelonephritis in experimental animals by reducing inflammatory markers and restoring antioxidant enzyme levels. Similarly,

investigations by Kamurthy et al. (2014), Mengi and Bakshi (2009), and Vysakh et al. (2020) demonstrated that aqueous root extracts of *R. aquatica* possess significant anti-inflammatory activity. The extracts effectively reduced inflammation in carrageenan-induced paw edema and crystal-induced inflammatory models, suggesting their potential application in the management of inflammatory disorders. Aswathanarayan and Vittal (2013) and Vysakh et al. (2020) reported that *Rotula aquatica* exhibits significant antibacterial activity against pathogenic microorganisms, including *Escherichia coli* and *Salmonella typhi*. Furthermore, the plant demonstrated antibiofilm activity against uropathogenic *E. coli*, suggesting its potential role in preventing and managing urinary tract infections and biofilm-associated complications.

Studies conducted by Ashwini C. S. et al. (2012), Bhanu Priya et al. (2014), and Shyam et al. (2013) demonstrated that both methanolic and aqueous extracts of *R. aquatica* possess significant antidiabetic activity in experimental diabetic rat models. Treatment with these extracts resulted in substantial reductions in blood glucose levels and significant improvements in lipid profiles, indicating their potential for glycemic control and metabolic regulation. Similarly, Gupta et al. (2011) and Singh et al. (2012) reported that alcoholic extracts of *R. aquatica* exhibit notable antidiarrheal and analgesic activities. Experimental studies revealed that the extracts effectively reduced pain responses in animal models and delayed the onset of diarrhea, thereby supporting their traditional medicinal use. Narayanan et al. (2022) investigated the nephroprotective potential of *R. aquatica* leaf extract using human embryonic kidney (HEK-293) cells and a gentamicin-induced nephrotoxicity rat model. The extract exhibited dose-dependent protective effects, with the 400 mg/kg treatment group showing significant improvements in renal function biomarkers and antioxidant enzyme levels. The protective effects were comparable to those of standard therapeutic agents, suggesting tha*t R. aquatica's* nephroprotective activity is attributable to its antioxidant and anti-inflammatory properties.

Agrawal et al. (2021) evaluated the antipyretic, analgesic, and anti-inflammatory activities of *R. aquatica* leaf extracts in experimental mouse and rat models. The methanolic extract exhibited significantly greater antipyretic, analgesic, and anti-inflammatory effects than the aqueous extract at a dose of 200 mg/kg. Pronounced analgesic activity was observed in hot plate and tail immersion assays. Furthermore, the methanolic extract significantly reduced paw edema in the carrageenan-induced inflammation model. These findings suggest that the extract may exert its anti-inflammatory effects by inhibiting the lipoxygenase pathway, although further mechanistic studies are required. The ethyl acetate fraction of *R. aquatica* (EFRA) has

been shown to effectively inhibit the growth of uropathogenic *Escherichia coli* and disrupt biofilm formation. Various in vitro studies demonstrated significant antibacterial activity, supported by its ability to damage bacterial cells and prevent biofilm development. These findings highlight the potential of EFRA as a natural therapeutic agent for the management of bacterial infections and biofilm-associated disorders (Vysakh et al., 2020). Phytochemical investigations have revealed that *R. aquatica* contains a diverse array of bioactive constituents, including triterpenoids (baurenol), steroids, alkaloids, rhabdiol, and allantoin (Vysak et al., 2016). Several studies have demonstrated the plant's antioxidant and antidiabetic potential (Priya et al., 2013; Sankh, 2010). Both methanolic and aqueous stem extracts have exhibited strong in vitro antioxidant activity, as evidenced by DPPH radical scavenging, superoxide radical scavenging, and reducing power assays. Furthermore, the high total phenolic and flavonoid contents of the extracts contribute significantly to their antioxidant properties (Priya et al., 2013). Collectively, these findings indicate that *R. aquatica* is a valuable source of bioactive phytochemicals with promising therapeutic applications in the prevention and management of various human diseases.

Shyam et al. (2013) evaluated the antidiabetic activity of methanolic root extracts of *Rotula aquatica* Lour. in streptozotocin-induced diabetic rats. The methanolic extract was administered orally at doses of 100, 200, and 400 mg/kg body weight, and its efficacy was compared with the standard antidiabetic drug glibenclamide (0.45 mg/kg body weight). Blood glucose levels and percentage reductions in blood glucose were assessed at different time intervals. Preliminary phytochemical screening was also performed to identify the major bioactive constituents. The results demonstrated that treatment with the methanolic root extract at a dose of 400 mg/kg body weight produced a significant reduction in blood glucose levels ($P < 0.01$) at 4 and 8 hours and a highly significant reduction ($P < 0.001$) at 8 hours. Phytochemical analysis revealed the presence of tannins and triterpenoids, which may contribute to the observed antidiabetic activity. Rameshwar et al. (2016) investigated the phytochemical composition of aqueous root extracts of *R. aquatica* using high-performance thin-layer chromatography (HPTLC). The analysis identified seven phenolic compounds, eleven saponins, and twelve tannins with distinct retention factor (Rf) values. These findings highlight the plant's rich phytochemical profile and suggest the need for further studies to isolate and characterise these compounds for potential therapeutic applications.

Phytochemical investigations have revealed the presence of several biologically active constituents in *R. aquatica*, including triterpenoids, steroids, alkaloids, rhabdiol, and allantoin.

These compounds are believed to contribute to the plant's diverse pharmacological activities. Previous studies have suggested its potential antidiabetic and antioxidant properties, warranting further investigation into its therapeutic applications. The ecological importance, economic value, and wide range of medicinal properties of *R. aquatica* underscore its significance as a promising resource for future research, herbal drug development, and sustainable conservation efforts.

Balan et al. (2016) reported the green synthesis of silver nanoparticles (AgNPs) using leaf extracts of *Lonicera japonica*. The synthesised nanoparticles exhibited excellent stability, structural integrity, and potent antioxidant activity. Furthermore, the AgNPs effectively inhibited α-amylase and α-glucosidase through reversible non-competitive inhibition, indicating promising antidiabetic potential. These findings suggest that *L. japonica*-mediated silver nanoparticles may serve as effective nanotherapeutic agents for diabetes management.

Mechchate et al. (2021) investigated the antidiabetic effects of *Withania frutescens* extract in diabetic mice over a four-week treatment period. The extract produced a significant long-term reduction in blood glucose levels and exhibited a favourable safety profile, with protective effects on hepatic and renal function. The observed inhibition of α-amylase and α-glucosidase activities suggested that its antidiabetic mechanism may involve the regulation of postprandial glucose metabolism. These findings support the potential use of *W. frutescens* as a natural therapeutic agent for long-term diabetes management.

Rehman et al. (2023) employed a green synthesis approach using *Azadirachta indica* seed extract to produce silver nanoparticles (AI-AgNPs) and evaluate their antidiabetic activity. The synthesised nanoparticles were characterised using Fourier-transform infrared spectroscopy (FTIR), scanning electron microscopy (SEM), dynamic light scattering (DLS), X-ray diffraction (XRD), and UV–visible spectroscopy. The antidiabetic potential of AI-AgNPs and crude seed extracts was assessed through glucose adsorption assays, glucose uptake by yeast cells, and α-amylase inhibition studies. The results demonstrated that the biosynthesised nanoparticles exhibit enhanced antidiabetic activity compared with the crude extracts. Similarly, Balan et al. (2016) described the eco-friendly synthesis of silver nanoparticles using *Lonicera japonica* leaf extract. A visible color change from pale yellow to dark brown confirmed nanoparticle formation. UV–visible spectroscopic analysis revealed a characteristic surface plasmon resonance peak at 435 nm, confirming the successful synthesis of silver nanoparticles.

Khattak (2019) reported the green synthesis of silver nanoparticles using *Quercus semecarpifolia* leaf extract. The synthesised nanoparticles were predominantly spherical and ranged from 20 to 50 nm in size, as confirmed by multiple characterisation techniques. The nanoparticles exhibited a crystalline structure and demonstrated significant biological activities, including strong antioxidant, cytotoxic, and phytotoxic effects. These findings indicate their potential applications in biomedical and environmental fields. Anju et al. (2021) demonstrated the green synthesis of silver nanoparticles using *Aloe vera* gel extract. Bioactive compounds such as acemannan acted as natural reducing and stabilising agents during nanoparticle formation. The synthesised nanoparticles exhibited enhanced antimicrobial activity against both Gram-positive and Gram-negative bacteria. The synergistic interaction between silver nanoparticles and plant-derived capping agents was found to contribute significantly to their biological efficacy, highlighting their potential for various biomedical applications.

Perumalsamy and Krishnadhas (2022) synthesised silver nanoparticles using hydroethanolic seed extracts of *Myristica fragrans* and evaluated their antidiabetic potential. Nanoparticle formation was achieved by mixing the extract with silver nitrate solution and exposing the mixture to sunlight. Characterisation studies confirmed nanoparticle synthesis, with UV–visible spectroscopy showing a characteristic absorption peak at 430 nm. In vitro antidiabetic assays revealed that the synthesised nanoparticles significantly inhibited α-amylase and α-glucosidase activities and reduced glucose diffusion and transport across membranes, indicating their potential for glycemic control.

The reviewed literature clearly demonstrates that diabetes mellitus remains one of the most challenging metabolic disorders worldwide, emphasising the need for safer and more effective therapeutic interventions. Although numerous synthetic antidiabetic drugs are available, their prolonged use is often associated with undesirable side effects. Consequently, medicinal plants have attracted considerable attention for their therapeutic efficacy, natural origin, and relatively lower incidence of adverse effects. In parallel, advances in nanotechnology, particularly the green synthesis of silver nanoparticles using plant extracts, have opened new avenues for the development of novel bioactive nanomaterials. Plant-mediated silver nanoparticles have been shown to possess enhanced antioxidant, antimicrobial, and antidiabetic activities due to the synergistic effects of phytochemicals and nanoscale materials. *Rotula aquatica* is a medicinally important plant rich in bioactive phytochemicals and has long been used in traditional systems of medicine. Although previous studies have documented its antioxidant, anti-inflammatory,

nephroprotective, and antidiabetic properties, limited attention has been given to its application in nanoparticle-mediated antidiabetic therapy. While green-synthesised silver nanoparticles derived from various medicinal plants have demonstrated promising antidiabetic potential, comparable studies involving *R. aquatica* remain scarce. In particular, systematic investigations evaluating the in vitro antidiabetic activity of *R. aquatica*-mediated silver nanoparticles have been inadequately explored.

Furthermore, limited information is available regarding the influence of nanoparticle characteristics on their biological activity. Consequently, a significant research gap exists concerning the synthesis, characterisation, and in vitro evaluation of silver nanoparticles derived from *R. aquatica*. Although several studies have reported the antidiabetic potential of medicinal plant extracts and plant-mediated silver nanoparticles, scientific evidence regarding *R. aquatica* based nanoparticles remains insufficient. Specifically, comprehensive investigations assessing their inhibitory effects on key carbohydrate-hydrolysing enzymes, such as α-amylase and α-glucosidase, are lacking. Addressing this research gap is essential for understanding the therapeutic potential of *R. aquatica*-mediated silver nanoparticles and exploring their possible application in diabetes management. Therefore, the present study was undertaken to synthesise silver nanoparticles using R. aquatica root extract through a green synthesis approach, characterise the synthesised nanoparticles, and evaluate their in vitro antidiabetic activity. The findings are expected to contribute to the growing field of plant-based nanotechnology and provide valuable insights for the development of novel antidiabetic nanotherapeutics.

Chapter 3
Aim and Objectives

3.1 Aim

To synthesise, characterise, and evaluate the *in vitro* antidiabetic potential of green-synthesised silver nanoparticles (AgNPs) from *Rotula aquatica* root extract.

3.2 Objectives

1. To synthesise *Rotula aquatica* mediated silver nanoparticles using a green synthesis approach.
2. To characterise the synthesised silver nanoparticles using physicochemical techniques.
3. To evaluate the *in vitro* cytotoxicity of the synthesised AgNPs using the MTT assay.
4. To assess the *in vitro* antidiabetic activity through α-amylase inhibition and glucose uptake assays.
5. To analyse GLUT 4 gene expression in treated and untreated L6 cells using qRT-PCR.

Chapter 4

Materials and Methods

4.1 Materials

4.1.1 Plant Material Selected for the Study

Fresh, healthy roots of *Rotula aquatica* were collected from Kollam District, Kerala, and used as plant material for the present study.

4.1.2 Cell Lines Used for the Study

The human liver cell line (HepG2) and rat skeletal muscle cell line (L6) were selected for the *in vitro* evaluation of antidiabetic activity.

4.1.3 Laboratory Materials and Consumables Used

The materials and consumables used in the present study included T25 culture flasks, 96-well plates, 6-well plates, micropipette tips, Eppendorf tubes, PCR tubes, Whatman No. 1 filter paper, and sterile centrifuge tubes.

4.2 Reagents

4.2.1 Reagents for Green Synthesis of Silver Nanoparticles

- 1 mM silver nitrate ($AgNO_3$) solution: Prepared by dissolving 0.085 g of $AgNO_3$ in 500 mL of distilled water.

4.2.2 Reagents for Cytotoxicity Screening

- Dulbecco's Modified Eagle Medium (DMEM) supplemented with 10% fetal bovine serum (FBS)
- Antibiotic solution (1%)
- Phosphate-buffered saline (PBS)
- Dimethyl sulfoxide (DMSO)
- Doxorubicin (standard drug, MW: 579.98 g/mol)
- MTT reagent (5 mg/mL in PBS)
- Detergent solution (50% DMF + 20% SDS)

4.2.3 Reagents for α-Amylase Inhibition Assay

- α-Amylase enzyme solution
- Starch substrate solution
- Sodium phosphate buffer (pH 6.9)
- 3,5-Dinitrosalicylic acid (DNSA) reagent
- Sodium potassium tartrate solution
- Metformin (reference standard, 10mg/ml)
- Distilled water

4.2.4 Reagents for Glucose Uptake Assay

- ab136955 Glucose uptake assay kit (colorimetric) (Abcam, USA)

Glucose uptake assay kit component reagents: -

- Assay Buffer 3
- Extraction Buffer
- Neutralisation Buffer II
- Enzyme Mix III
- Glutathione reductase
- Recycling Mix
- DTNB (5,5′-Dithiobis-(2-nitrobenzoic acid))
- 2-Deoxyglucose (2-DG)
- 2-DG6P Standard

Krebs–Ringer–Phosphate–HEPES (KRPH) buffer containing:

- 20 mM HEPES
- 5 mM KH_2PO_4
- 1 mM $MgSO_4$
- 1 mM $CaCl_2$
- 136 mM NaCl
- 4.7 mM KCl
- pH 7.4
- 2% bovine serum albumin (BSA)

4.2.5 Reagents for RNA Isolation

- TRIzol reagent (Sigma, USA)
- Chloroform
- Ethanol (75%)
- DEPC-treated water
- Nuclease-free water

4.2.6 Reagents for cDNA Synthesis and Quantitative PCR

- iScript cDNA Synthesis Kit (Bio-Rad, USA)
- SYBR® Green Master mix (Bio-Rad, USA)
- Forward and reverse primers (Glut 4 and GAPDH)

4.3 Instruments

The instruments used in the present study included:

- Dynamic Light Scattering (DLS) analyser (Anton Paar)
- UV–Visible spectrophotometer (Thermo scientific, USA)
- Fourier Transform Infrared (FTIR) spectrophotometer (Shimadzu)
- Centrifuge (Eppendorf, Germany)
- Analytical weighing balance (shimadzu, Japan)
- Hot air oven (Thermo Fischer Scientific, USA)
- Magnetic stirrer (Bionics scientific)
- pH meter (Grant instruments, UK)
- Autoclave (Bionics scientific)
- Water bath (Grant instruments, UK)
- Gel electrophoresis apparatus (Bio-Rad, USA)
- Haemocytometer (Thermo Fischer scientific)
- CO_2 incubator (Thermo Fischer scientific)
- Microplate reader (Bio Tek 800 TS, USA)
- CFX-96 RealTime System (Bio-Rad, USA)

4.4 Methodology

4.4.1 Collection and Identification of Plant Material

Fresh and healthy roots of *Rotula aquatica* were collected from Kollam District, Kerala. The collected plant material was thoroughly washed under running tap water, followed by rinsing with distilled water to remove adhering soil particles and other impurities. The roots were then shade-dried at room temperature and ground into a fine powder using a mixer grinder. The powdered material was stored in airtight containers at 4°C until further use.

4.4.2 Green Synthesis of Silver Nanoparticles

4.4.2.1 Preparation of Aqueous Root Extract

Four grams of *Rotula aquatica* root powder were mixed with 100 mL of distilled water in a conical flask. The mixture was heated at 70°C for 20 minutes with continuous stirring. After cooling to room temperature, the extract was filtered through Whatman No. 1 filter paper to remove particulate matter. The resulting aqueous extract was collected and stored at 4°C until further use.

4.4.2.2 Biosynthesis of Silver Nanoparticles Using *Rotula aquatica* Root Extract

For the synthesis of silver nanoparticles, the aqueous root extract was brought to room temperature. A 20 mL aliquot of the extract was mixed with 180 mL of 1 mM silver nitrate ($AgNO_3$) solution and stirred continuously for 10 minutes. The reaction mixture was then incubated overnight at room temperature.

The formation of silver nanoparticles was initially indicated by a colour change from pale yellow to reddish-brown due to the reduction of silver ions and the subsequent formation of silver nanoparticles. The synthesis was further confirmed by UV–Visible spectrophotometer analysis.

The reaction mixture was centrifuged at 6000 rpm for 20 minutes, and the resulting pellet was collected. The pellet was washed twice with distilled water to remove any unreacted components and impurities. The purified nanoparticles were dried in a hot-air oven and stored in airtight containers for further characterisation and biological evaluation.

4.5 Characterisation of Silver Nanoparticles

4.5.1 UV–Visible Spectrophotometer Analysis

The formation and stability of silver nanoparticles synthesised from *Rotula aquatica* root extract were confirmed using a UV–Visible spectrophotometer. This technique is based on surface plasmon resonance (SPR), a characteristic optical property of metallic nanoparticles that provides information on particle formation, size distribution, and stability.

The synthesised silver nanoparticle suspension was placed in a quartz cuvette, and the absorption spectrum was recorded over 300–700 nm. The appearance of a characteristic SPR absorption peak within this range confirmed the formation of silver nanoparticles.

4.5.2 Dynamic Light Scattering (DLS) Analysis

The hydrodynamic particle size distribution of the synthesised silver nanoparticles was determined using Dynamic Light Scattering (DLS) analysis with a Litesizer instrument.

The nanoparticles were dispersed in deionised water to form a colloidal suspension, then sonicated for 15 minutes to ensure uniform dispersion and minimise particle aggregation. Approximately 1 mL of the suspension was filtered through a 0.22 μm syringe filter to remove larger particles and contaminants that could interfere with the measurements.

The filtered suspension was transferred to a clean disposable cuvette and analysed at room temperature (25°C). Measurements were performed at a scattering angle of 90°. The instrument measured fluctuations in the intensity of scattered light caused by the Brownian motion of nanoparticles, which were subsequently used to calculate the hydrodynamic diameter and size distribution of the synthesised nanoparticles.

4.5.3 Fourier Transform Infrared (FTIR) Spectroscopic Analysis

Fourier Transform Infrared (FTIR) spectroscopy was employed to identify the functional groups associated with the synthesised silver nanoparticles and to determine the phytochemical constituents responsible for nanoparticle reduction and stabilisation.

Dried silver nanoparticle samples were subjected to FTIR analysis using an FTIR spectrometer. Spectra were recorded over a wavenumber range of 4000–400 cm^{-1} at a resolution of 4 cm^{-1}. The obtained spectra were analysed to identify characteristic absorption bands corresponding to various functional groups present on the nanoparticle surface. The results provided

information regarding the biomolecules involved in the synthesis, capping, and stabilisation of the silver nanoparticles.

4.6 Cell Viability Assay

4.6.1 MTT Assay

The cytotoxic effects of *Rotula aquatica*-mediated silver nanoparticles on L6 skeletal muscle cells and HepG2 hepatic cells were evaluated using the MTT assay. Cells were seeded at a density of 1×10^4 cells per well in 96-well plates and incubated overnight under standard culture conditions to allow cell attachment.

Upon reaching approximately 70–80% confluency, the cells were treated with different concentrations (10, 25, 50, 75, and 100 µg/mL) of *Rotula aquatica* silver nanoparticles prepared in Dulbecco's Modified Eagle Medium (DMEM). The treated cells were incubated for 24 h at 37°C in a humidified atmosphere containing 5% CO_2.

After incubation, 100 µL of MTT reagent (5 mg/mL in PBS) was added to each well, and the plates were incubated in the dark at 37 °C for 2 h. Subsequently, 100 µL of detergent solution (50% DMF and 20% SDS) was added to each well to dissolve the purple formazan crystals formed by viable cells. After a further 2 h of incubation, the absorbance was measured at 570 nm using a microplate reader.

Cell viability was calculated using the following formula:

$$\text{Cell Viability (\%)} = \frac{\text{Absorbance of treated cells}}{\text{Absorbance of control cells}} \times 100$$

4.7 Antidiabetic Assays

4.7.1 α-Amylase Inhibition Assay

The α-amylase inhibitory activity of *Rotula aquatica* silver nanoparticles was evaluated using an in vitro enzyme inhibition assay. Different concentrations of the sample (50-250 µg/mL) were prepared in suitable reaction tubes.

To each tube, 100 µL of α-amylase enzyme solution (0.5 mg/mL) was added and incubated at 25°C for 10 min. Subsequently, 100 µL of 1% soluble starch solution prepared in sodium phosphate buffer (pH 6.9) was added and incubated for an additional 10 min at 25°C.

The reaction was terminated by adding 200 µL of 3,5-dinitrosalicylic acid (DNSA) reagent. The tubes were then placed in a boiling water bath at 100°C for 5 min to develop color. After cooling to room temperature, 2 mL of distilled water was added to each tube. A control containing all reagents except the test sample was maintained under identical conditions.

The absorbance was measured at 540 nm using a UV–Visible spectrophotometer. Metformin was used as the reference standard. The percentage inhibition of α-amylase activity was calculated using the following formula:

$$\text{Inhibition (\%)} = \frac{\text{Absorbance of Control} - \text{Absorbance of Sample}}{\text{Absorbance of Control}} \times 100$$

4.7.2 Glucose Uptake Assay

4.7.2.1 Preparation of Reagents and Standards

Glucose uptake was quantified using a commercial Glucose Uptake Assay Kit (Colorimetric) (ab136955, Abcam, USA). Prior to use, all kit components were equilibrated to room temperature and centrifuged briefly.

The lyophilized reagents were reconstituted according to the manufacturer's instructions. Enzyme Mix III was dissolved in 220 µL of Assay Buffer 3 and kept on ice. Glutathione reductase was dissolved in 1.1 mL of Assay Buffer 3, while the Recycling Mix was reconstituted in 220 µL of Assay Buffer 3. DTNB reagent was dissolved in 1 mL of Assay Buffer 3. Reconstituted reagents were aliquoted and stored at −20°C until use.

The 2-deoxyglucose-6-phosphate (2-DG6P) standard was reconstituted with 100 µL of ultrapure water to obtain a 10 mM stock solution. Serial dilutions were prepared to generate a standard curve containing 0, 20, 40, 60, 80, and 100 pmol of 2-DG6P per well in a final volume of 50 µL. All standards were prepared in duplicate.

4.7.2.2 Cell Seeding, Starvation, and Treatment

L6 cells were seeded in sterile 96-well plates at a density of 1.5×10^3 cells per well in 100 µL of complete culture medium. After reaching the desired confluency, the cells were washed twice with phosphate-buffered saline (PBS) and incubated overnight in serum-free medium to induce glucose starvation.

On the following day, the cells were washed three times with PBS and incubated in 100 µL of Krebs–Ringer–Phosphate–HEPES (KRPH) buffer containing 2% bovine serum albumin

(BSA) for 40 min at 37°C to further deplete intracellular glucose reserves. The KRPH buffer consisted of 20 mM HEPES, 5 mM KH_2PO_4, 1 mM $MgSO_4$, 1 mM $CaCl_2$, 136 mM NaCl, and 4.7 mM KCl (pH 7.4).

The experimental groups were arranged as follows:

- **Sample Background Control:** Glucose-starved cells were washed with PBS and lysed immediately without exposure to 2-deoxyglucose (2-DG).
- **Insulin-Stimulated Positive Control:** Cells were treated with 1 μM insulin for 20 min prior to the addition of 2-DG.
- **Test Samples:** Cells were treated with different concentrations (10, 25, 50, 75, and 100 μg/mL) of *Rotula aquatica* silver nanoparticles prepared in KRPH buffer containing 2% BSA for 20 min.

Untreated Control: Cells received KRPH buffer alone without insulin or sample treatment. Following treatment, 10 μL of 10 mM 2-deoxyglucose (2-DG) was added to each well, and the cells were incubated for an additional 20 min at 37°C. After incubation, the cells were washed 3 times with PBS to remove extracellular and unabsorbed 2-DG, then lysed, and intracellular glucose uptake was quantified according to the manufacturer's protocol.

4.7.2.3 Endogenous NAD(P) Degradation and Cell Lysis

To release intracellular components and eliminate endogenous NAD(P), while simultaneously denaturing endogenous enzymes, all experimental cell groups were lysed by repeated pipetting in 80 μL of Extraction Buffer I. The resulting cell lysates were subjected to a single freeze–thaw cycle and subsequently incubated at 85°C for 40 min.

Following incubation, the lysates were cooled on ice for 5 min and neutralized by adding 10 μL of Neutralization Buffer II. The samples were then centrifuged briefly at approximately 500 rpm for 1–2 min, and the clear supernatants were transferred to fresh microcentrifuge tubes. When necessary, samples were diluted 1:10 with Assay Buffer 3 (5 μL sample + 45 μL Assay Buffer 3) to ensure that absorbance values fell within the linear range of the standard curve.

4.7.2.4 Reaction Assay and Spectrophotometric Measurement

For the enzymatic assay, 50 μL of each standard solution, sample background control, insulin-stimulated sample, untreated control, and test sample was added to the designated wells of a 96-well microplate.

A master Reaction Mix A was prepared for NADPH generation by combining 8 µL of Assay Buffer 3 and 2 µL of Enzyme Mix III per reaction. Subsequently, 10 µL of Reaction Mix A was added to each well. The plate was mixed thoroughly and incubated at 37°C for 1 h.

To degrade residual unreacted NADP, 90 µL of Extraction Buffer I was added to each well. The plate was sealed with aluminium sealing film and heated at 90°C for 40 min. After heating, the plate was cooled on ice for 5 min and neutralised by adding 12 µL of Neutralisation Buffer II to each well.

A master Reaction Mix B was then prepared for the recycling amplification reaction by combining:

- 20 µL Glutathione Reductase
- 16 µL DTNB
- 2 µL Recycling Mix per reaction.

A volume of 38 µL of Reaction Mix B was added to each well, and the mixture was thoroughly mixed by gentle pipetting.

The absorbance was measured at 412 nm using a microplate reader operating in kinetic mode at 37°C and protected from direct light. Readings were recorded every 2–3 min until the absorbance of the highest standard (100 pmol/well) reached an optical density (OD) of approximately 1.5–2.0. Subsequently, a final endpoint absorbance reading was recorded for all standards and samples.

4.7.2.5 Data Analysis

All standards, controls, and experimental samples were analysed in triplicate. The mean absorbance values were calculated, and the blank standard absorbance (0 pmol 2-DG6P) was subtracted from all readings to obtain corrected absorbance values. For experimental samples, the absorbance values obtained from the sample background controls (cells not exposed to insulin or 2-deoxyglucose) were subtracted to eliminate background interference. A standard calibration curve was generated by plotting the corrected absorbance values against the corresponding concentrations of 2-DG6P (0–100 pmol).

A best-fit regression equation was obtained from the standard curve and used to interpolate the amount of intracellular 2-DG6P present in each sample well. The quantity of glucose uptake was calculated using the following equation:

$$\text{2-DG Uptake} = \left(\frac{T_s}{S_v}\right) \times D \text{where:}$$

- **Ts** = Amount of 2-DG6P in the sample well interpolated from the standard curve (pmol)
- **Sv** = Initial sample volume loaded into the reaction well (µL)
- **D** = Dilution factor applied to the sample prior to analysis

The calculated values were expressed as pmol of 2-deoxyglucose uptake per microliter of sample and used to compare glucose uptake among the different treatment groups.

4.8 RNA Isolation

All materials used for RNA isolation were treated with 0.01% diethyl pyrocarbonate (DEPC) and incubated at room temperature overnight. Treated materials were then autoclaved to destroy any residual DEPC. All reagents were prepared with DEPC- treated water to inactivate RNases. The RNA isolation workspace, pipettes, plasticware, and centrifuge were wiped twice with RNaseZap to eliminate surface RNases.

Procedure

Total RNA was isolated using TRIzol reagent according to the manufacturer's instructions (Invitrogen), and the extracted RNA was stored at -80°C (Thermo Scientific, USA).

- Based on the highest glucose uptake concentration the cells were treated with 100 µg/mL of *Rotula aquatica* mediated silver nanoparticles for 24hrs.
- Cells were collected for RNA isolation using 1 mL TRIzol under aspetic conditions in a laminar air flow hood.
- Aspirated the media from the well, and 1 ml of TRIzol reagent was added directly to the well to lyse the cells.
- Following lysis, the lysate was transferred to an Eppendorf tube and stored at -80°C.
- The sample was vortexed and incubated at room temperature for 5 min.
- Chloroform (200 µL) was added to each sample, followed by vigorous shaking for seconds and incubation at room temperature for 3 minutes.
- The samples were centrifuged at 12,000 × g for 15 minutes at 4°C, and the upper aqueous phase containing RNA was carefully transferred to a new tube.
- RNA was precipitated by adding 500 µL of isopropanol and then gently mixing it before incubating at room temperature for 10 minutes.
- The samples were then subjected to centrifugation at 12,000 × g for 10 minutes at a

temperature of 4°C.

- Removed the supernatant and washed the pellet with 1 mL 75% ethanol (diluted with DEPC water).
- Vortexed once and centrifuged at 2000 rpm for 4 min at 4°C.
- Discarded the supernatant, and the pellet was dried for 5 min at room temperature.
- Dissolved pellet in DEPC water and stored at -20°C.

The RNA concentration and purity were measured using a Biophotometer (Eppendorf, USA), and RNA integrity was assessed by 1.2% agarose gel electrophoresis. Samples with an A260/A280 ratio between 1.8 and 2.1 and clear rRNA bands were chosen for the next step of cDNA synthesis.

4.9 cDNA synthesis

Using the iScript™ cDNA Synthesis Kit (Bio-Rad Laboratories, USA) according to the manufacturer's instructions, first-strand complementary DNA (cDNA) was produced from 1µg of total RNA. 4 µL of 5× iScript Reaction Mix, 1 µL of iScript Reverse Transcriptase, 1µg of RNA template, and nuclease-free water were added to the reaction mixture (20 µL total volume).

The reaction was incubated in a thermal cycler with the following conditions:

25 °C for 5 minutes (primer annealing)
46 °C for 20 minutes (reverse transcription)
95 °C for 1 minute (inactivation of reverse transcriptase)

The synthesized cDNA was stored at -20 °C and diluted 10 times before use in qPCR reactions.

4.10 Primers used for the study

The primer sequences used for quantitative real-time PCR (qRT-PCR) analysis were as follows: for the GLUT 4 gene, the forward primer sequence was 5′-GGT CTC CTC TGA CTT CAA CA-3′ and the reverse primer sequence was 5′-AGC CAA ATT CGT TGT CAT AC-3′. GAPDH was used as the reference (housekeeping) gene, with the forward primer sequence 5′-CCATCCTGATGACTGTGGCTCT-3′ and the reverse primer sequence 5′-GCCACGATGAACCAAGGAATGG-3′. The annealing temperature of the primers was optimized by gradient PCR over a temperature range of 56–60°C.

4.11 Quantitative Real-Time PCR (qPCR)

Quantitative Real-Time PCR (qPCR) was performed for gene expression analysis using SYBR Green-based chemistry on a Bio-Rad CFX96 system (Bio-Rad Laboratories, USA). The 20 µL reaction mixture included 2 µL of 10x diluted cDNA, 10 µL of 2X SYBR Green Master Mix (2x). Quantitative Real-Time PCR (qPCR) was performed for gene 5 µL each of forward and reverse primers (10 picomoles), and nuclease-free water to volume. The reaction was incubated in a thermal cycler with the following conditions:

- 95 °C for 3 minutes (initial denaturation)
- 40 cycles of: -

  95 °C for 10 seconds (denaturation)

  60 °C for 30 seconds (annealing**)**

  72 °C for 30 seconds (extension)

At the end of each run, melt curve analysis was performed to confirm the specificity of the amplified products.

4.11.1 Data Analysis

The relative expression levels of the target genes were determined using the 2^(-ΔΔCt) method (Livak and Schmittgen, 2001). The housekeeping gene was used as an internal reference for normalization. All reactions were performed in technical triplicate, and the mean Ct values were used for subsequent analysis. Fold changes in gene expression were calculated by comparing the Ct values of the samples with the control sample.

The relative expression of the Glut 4 gene was calculated using the following steps:

Step 1: Calculation of ΔCt

For each sample, the Ct value of the reference gene (GAPDH) was subtracted from the Ct value of Glut 4 gene.

$$\Delta Ct = Ct_{(target\ gene)} - Ct_{(gapdh)}$$

This normalization step corrects for sample-to-sample variations in template concentration.

Step 2: Calculation of ΔΔCt

The ΔCt value of each test sample was compared with the ΔCt value of the control sample to determine the relative change in expression:

$$\Delta\Delta Ct = \Delta Ct_{(Test)} - \Delta Ct_{(Control)}$$

The control sample served as the calibrator against which all other samples were evaluated.

Step 3: Calculation of Relative Gene Expression

The fold change in Glut 4 gene expression relative to the control was determined using the following equation:

$$\text{Relative Expression (Fold Change)} = 2^{-\Delta\Delta Ct}$$

A fold-change value greater than 1 indicated upregulation of Glut 4 expression relative to the control, whereas a value less than 1 indicated downregulation. A fold-change value equal to 1 represented no significant change in expression. The calculated relative expression values were used to compare Glut 4 transcript abundance between the control and treated samples. The results were expressed as mean fold-change values derived from three technical replicates and were subsequently used for statistical analysis and graphical representation.

4.11.2 Statistical Analysis

All RealTime-PCR reactions were performed in triplicates. Mean Ct values were used for the calculation of ΔCt, ΔΔCt, and fold-change values. Results were expressed as mean ± standard error (SE). Statistical analyses and graphical representations were performed using Microsoft Excel.

Chapter 5

Results

5.1 Green Synthesis of Silver Nanoparticles Using *Rotula aquatica* Root Extract

The formation of silver nanoparticles was initially confirmed by a visible colour change in the reaction mixture. Upon the addition of *Rotula aquatica* root extract to the silver nitrate solution, the colour of the solution changed from pale yellow to reddish-brown (Figure 2). The reddish-brown colour indicated the formation of silver nanoparticles.

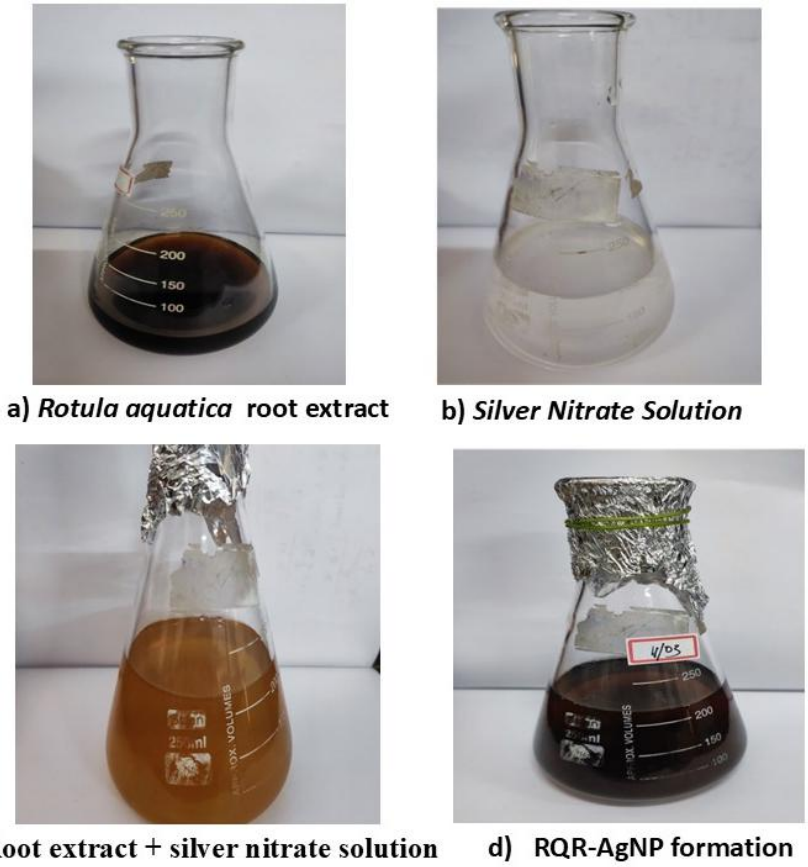


Figure 2: Stages of silver nanoparticle synthesis from root extract

5.2 Characterization of silver nanoparticles

5.2.1 UV-Vis spectrophotometer

The synthesis of silver nanoparticles (AgNPs) using *Rotula aquatica* root extract was confirmed by UV–Visible (UV–Vis) spectrophotometric analysis. The UV–Vis absorption spectrum of *Rotula aquatica* root extract-mediated AgNPs (RQR-AgNPs) exhibited a characteristic absorption peak at 447 nm, corresponding to the surface plasmon resonance

(SPR) of silver nanoparticles (Figure 3). The appearance of this distinct SPR band is a well-established indicator of AgNP formation, confirming the successful green synthesis of silver nanoparticles using *Rotula aquatica* root extract. Typically, the SPR absorption peak of silver nanoparticles is observed within the range of 400–450 nm, and the observed peak at 447 nm is consistent with the characteristic optical properties of AgNPs.

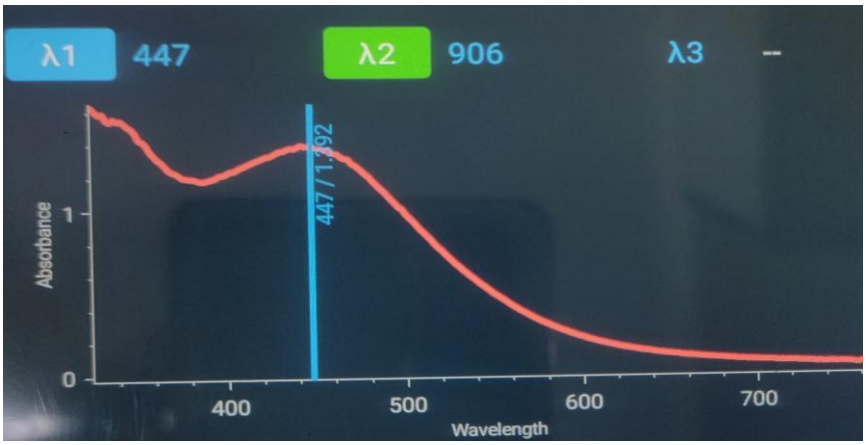


Figure 3: - UV -Visible absorption spectrum of RQR-AgNPs

5.2.2 Fourier Transform Infra-Red Spectroscopy (FTIR)

FTIR spectroscopy was performed to identify the functional groups of biomolecules involved in the reduction of Ag^{+} ions and capping of silver nanoparticles. A broad absorption band observed at 3269.63 cm^{-1} corresponds to O-H stretching vibrations linked to intermolecular hydrogen bonding, suggesting the existence of phenolic and alcoholic –OH groups deriving from the capping substances. A distinct peak found at 3726.75 cm^{-1} is indicative of free O-H stretching, likely due to water molecules that are adsorbed. The peak located at 2980.61 cm^{-1} relates to the aliphatic C-H stretching vibrations from CH_2/CH_3 groups (Figure 4).

The band at 1617.45 cm^{-1} is attributed to C=O stretching/amide I vibrations, implicating the role of proteins or peptides in the stabilization of the nanoparticles. The peak at 1381.22 cm^{-1} signifies C-H bending vibrations, while the band at 1250.93 cm^{-1} corresponds to C-O stretching from carboxylic or phenolic groups. In the fingerprint region, the prominent peaks at 1149.36, 1076.02, and 1015.93 cm^{-1} are attributed to C-O-C stretching vibrations due to polysaccharides and flavonoids, which affirm their function as reducing and stabilizing agents for AgNPs. The minor bands at 2185.31, 2112.21, 2010.83, and 1952.62 cm^{-1} relate to C≡C/C≡N stretching vibrations arising from trace phytoconstituents. Key peaks confirming AgNP presence are

observed below 600 cm^{-1} at 571.07, 473.76, 463.49, 425.65, and 415.19 cm^{-1}. These bands signify Ag-O stretching vibrations, thus confirming the formation of metallic silver nanoparticles and their interaction with the biomolecules present on the nanoparticle surface.

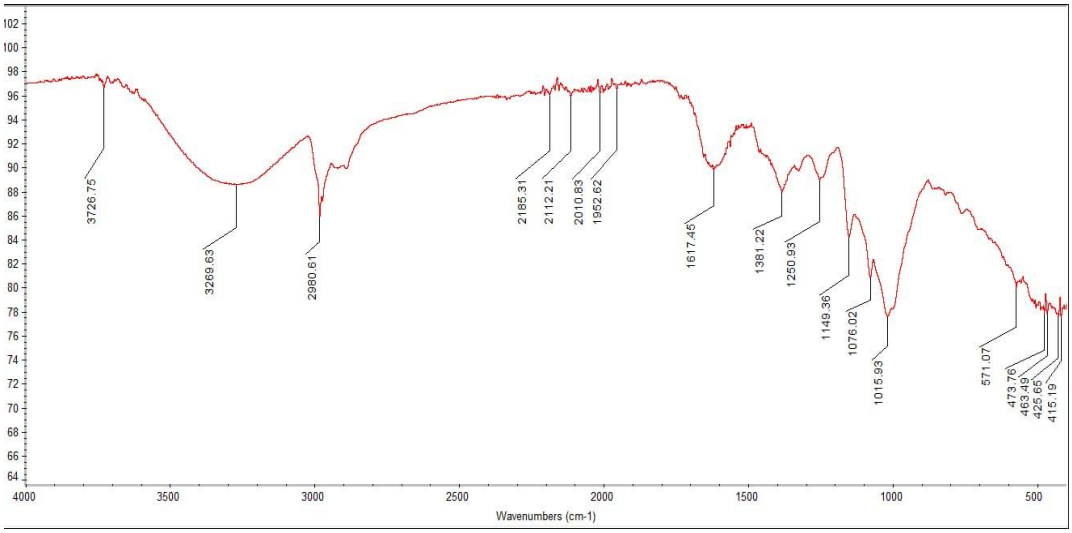


Figure 4: FTIR spectrum of RQR - AgNP

5.2.3 Dynamic Light Scattering Analysis

Dynamic Light Scattering (DLS) analysis was performed to determine the particle Size distribution of the synthesized silver nanoparticles. The DLS profile exhibited a single, narrow peak with a hydrodynamic diameter of approximately 45–50 nm, indicating the formation of uniformly sized nanoparticles (Figure 5). The absence of additional peaks or larger particle populations suggests minimal aggregation and confirms the suspension's homogeneity. Furthermore, the steep cumulative undersize curve indicates a narrow size distribution and good colloidal dispersion. These results demonstrate the successful synthesis of stable, uniform silver nanoparticles, making them suitable for potential biomedical, pharmaceutical, and antimicrobial applications.

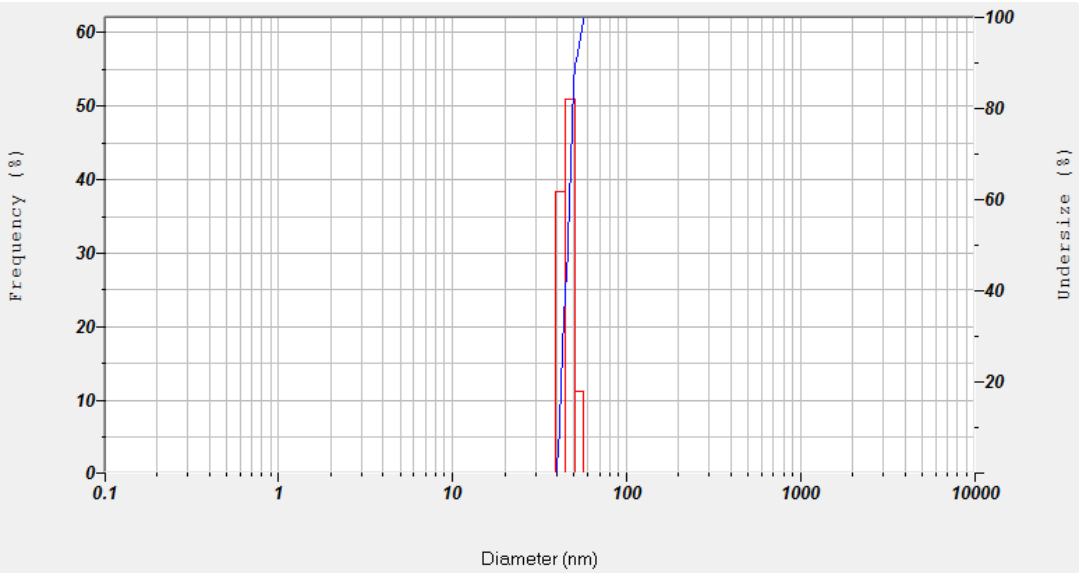


Figure 5: size range of RQR silver nanoparticles obtained by DLS analysis

5.3 MTT Assay

5.3.1 Assessment of Cytotoxic effects using *Rotula aquatica* mediated silver nanoparticles in HepG2 cell line

After measuring the optical density of each well, the cell viability is calculated. The percentage of cell viability was calculated using the following formula:-

Cell viability (%) = (Mean OD of test-Mean OD of blank)/(Mean OD of Vehicle control-Mean OD of blank) ×100

Table 2: Dose-Dependent reduction in HepG2 cell viability

Group	%Viability	SD	Interpretation
Control	100	0.009	Normal untreated cell
Positive control (Doxorubicin 3.5µg/ml)	10.25	0.006	Potent cytotoxic effect
10 µg/ml	69.13	0.008	Mild Toxicity
25 µg/ml	54.89	0.011	Moderate Toxicity
50 µg/ml	42.24	0.007	Significant Cytotoxicity
75 µg/ml	34.28	0.012	High Cytotoxicity
100 µg/ml	29.88	0.01	Severe Cytoxicity

The cytotoxicity of the test compound was evaluated in HepG2 cells using a cell viability assay, as shown in Table 2. The untreated control group was considered 100% viable, while the positive control showed a marked reduction in cell viability (10.25%). Treatment with the test

compound resulted in a dose-dependent decrease in HepG2 cell viability. These findings suggest that the compound is safe at lower concentrations, whereas higher concentrations significantly reduce HepG2 cell viability (Figure 6).

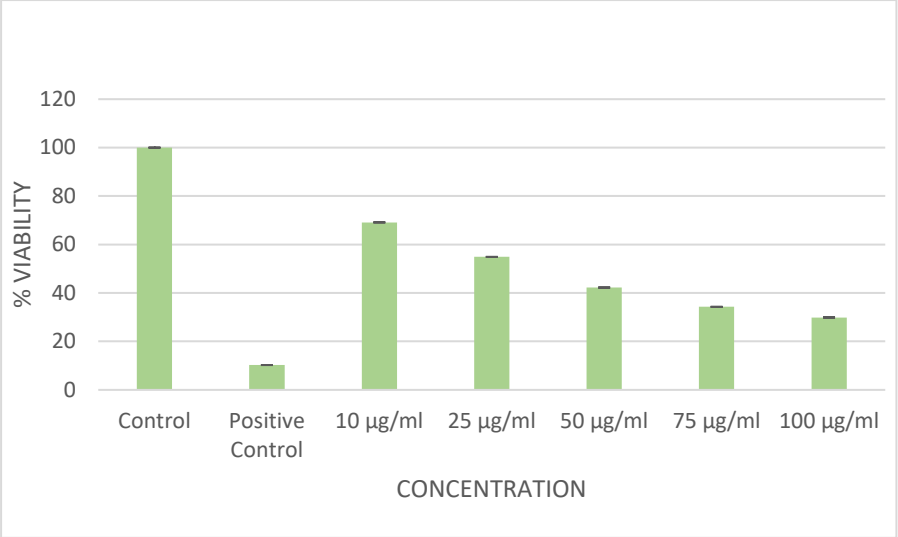


Figure 6: Dose-dependent effect of *Rotula aquatica* mediated silver nanoparticle on HepG2 cell Viability

Therefore, concentrations below 25 µg/ml may be considered safer for antidiabetic investigations, whereas concentrations of 75 µg/ml or higher exhibit substantial cytotoxicity. Data are presented as the mean, Standard deviation (SD) from independent experiments. The half-maximal inhibitory concentration (IC50) was determined from the data as mentioned in Table 3, and a dose-response curve was generated using percentage cell viability data (Figure 7). The calculated % cell viability values were plotted on the Y-axis against the drug concentrations on the X-axis to obtain a sigmoidal dose-response curve. The IC50 value was determined as the concentration corresponding to 50% inhibition (i.e., 50% cell viability) from the fitted curve.

Table 3: Cell viability of *Rotula aquatica* mediated silver nanoparticle against each concentration of drug in HepG2 cells.

Concentration	% Cell viability
10 µg/ml	69.13
25 µg/ml	54.89
34.7 µg/ml	**50**
50 µg/ml	42.24
75 µg/ml	34.28
100 µg/ml	29.88

.

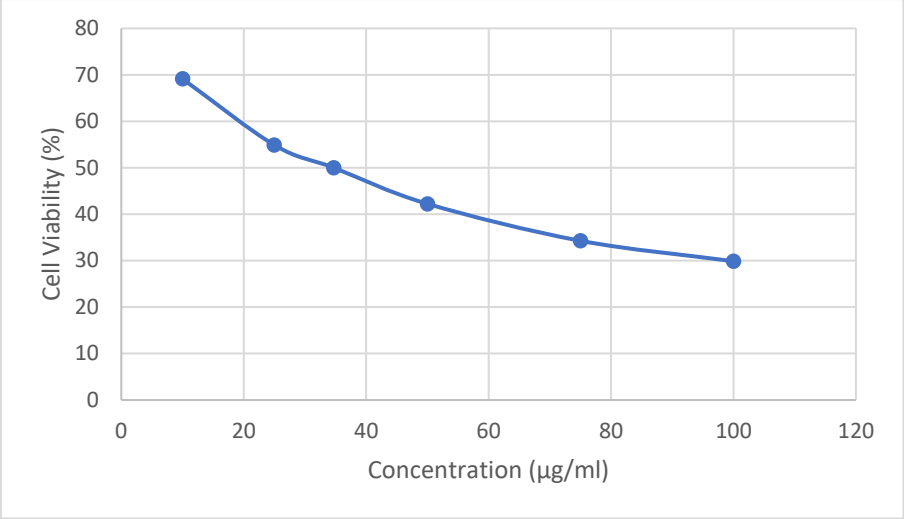


Figure 7: Graph plotting cell viability against various concentrations of *Rotula aquatica* mediated silver nanoparticles concentration (HepG2)

Calculated IC_{50} value was 34.7 µg/mL, indicating that this concentration reduced HepG2 cell viability by 50%. Doxorubicin was used as the standard drug for evaluating cytotoxicity activity. The reported IC_{50} range of doxorubicin for HepG2 cells was 0.5-12.5 µM, and 6 µM (approximately 3.5 µg/ml) was selected, and its cytotoxic activity was evaluated as shown in Table 4.

Table 4: Cytotoxicity evaluation of doxorubicin and *Rotula aquatica* mediated silver nanoparticles in HepG2 based on IC_{50} value

Treatment	HepG2 IC_{50}	Interpretation
Doxorubicin	3.5 µg/ml	Stronger cytotoxicity
RQR-AgNP	37.4 µg/ml	Moderate cytotoxicity

5.3.2 Assessment of Cytotoxic effects using *Rotula aquatica* mediated silver nanoparticles in L6 cell line

Table 5: Dose-Dependent reduction in L6 cell viability

Group	% viability	SD	Interpretation
Control	100	0.09	Normal untreated Cell
Positive control (Doxorubicin 8.7µg/ml)	10.25	0.06	Potently cytotoxic
10 µg/ml	77.77	0.08	Mild cytotoxic
25 µg/ml	62.05	0.07	Moderately Cytotoxic
50 µg/ml	54.27	0.09	Significant Toxicity
75 µg/ml	47.22	0.08	Toxic
100 µg/ml	37.22	0.06	Highly toxic

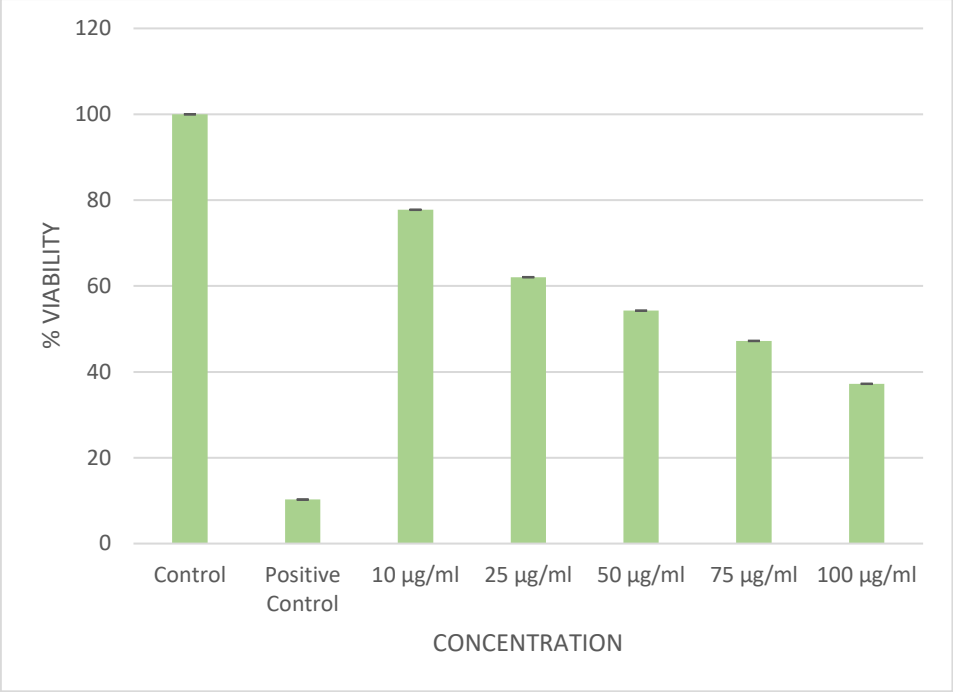


Figure 8: Dose-dependent effect of *Rotula aquatica-mediated* silver nanoparticles on L6 cell viability

The cytotoxicity of the test compound was evaluated in L6 skeletal muscle cells using a cell viability assay (Table 5). The untreated control exhibited 100% cell viability, whereas the positive control showed a substantial reduction in viability (10.25%), confirming the assay's sensitivity and reliability (Figure 8). Treatment with the test compound resulted in a concentration-dependent decrease in cell viability.

These findings indicate that the compound maintains acceptable cell viability at lower concentrations and may be considered relatively safe for antidiabetic evaluation in L6 skeletal muscle cells. However, increasing concentrations led to a progressive reduction in cell viability, suggesting a dose-dependent cytotoxic effect. Therefore, concentrations between 25 µg/ml appear most suitable for further antidiabetic activity studies, while concentrations of 75 µg/ml or higher should be used with caution due to their increased cytotoxicity. The half-maximal inhibitory concentration (IC50) was determined from the dose-response curve generated using percentage cell viability data. The calculated % cell viability values were plotted on the Y-axis against the drug concentrations on the X-axis to obtain a sigmoidal dose-response curve. The IC50 value was determined as the concentration corresponding to 50% inhibition (i.e., 50% cell viability) from the fitted curve.

Table 6: showing cell viability of *Rotula aquatica* mediated silver nanoparticle against each concentration of drug in L6 cells

Concentration	% cell viability
10 µg/ml	77.77
25 µg/ml	62.05
50 µg/ml	54.27
65.1 µg/ml	**50**
75 µg/ml	47.22
100 µg/ml	37.22

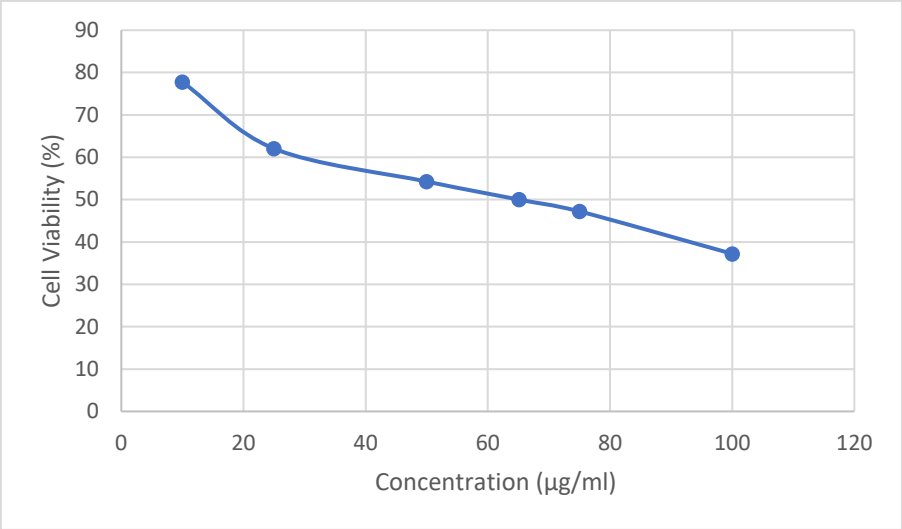


Figure 9: Graph plotting cell viability against various concentrations of *Rotula aquatica* mediated silver nanoparticles (L6)

The calculated IC_{50} value of 65.1 µg/mL, reported in Table 6, indicates that this concentration reduced L6 cell viability by 50% (Figure 9). Doxorubicin was used as the standard drug for evaluating cytotoxicity activity. The reported IC_{50} range of doxorubicin for L6 cells was 0.5-20 µM, and 15µM (8.7 µg/mL) was selected, and its cytotoxicity was evaluated as shown in Table 7.

Table 7: Cytotoxicity evaluation of doxorubicin and *Rotula aquatica* mediated silver nanoparticles in L6 based on IC_{50} value

Treatment	L6 IC_{50}	Interpretation
Doxorubicin	8.7 µg/mL	Stronger cytotoxicity
RQR-AgNP	65.1 µg/mL	Lower cytotoxicity

Since concentrations above 65.1 µg/mL cause significant cytotoxicity. Therefore, for antidiabetic evaluation, only concentrations well below 65.1 µg/mL can be considered for further glucose uptake studies. The test compound showed IC_{50} values of 34.7 µg/mL in HepG2 cells and 65.1 µg/mL in L6 cells. Since the IC_{50} value was higher in L6 cells, the compound was less cytotoxic to L6 skeletal muscle cells than to HepG2 liver cells. This indicates a better

safety profile in L6 cells and suggests that the compound may be suitable for antidiabetic studies at lower concentrations, particularly between 10 and 25 µg/mL where acceptable cell viability was observed.

5.4 Antidiabetic Assay

5.4.1 Alpha amylase inhibition assay

Inhibitory effects of the extract on α-amylase: Alpha-amylase catalyses the α-(1-4)-D-glycosidic linkages present in the starch, breaking them into polymers of glucose and other small fragments. Extracts were tested for their α-amylase inhibition using the spectrophotometric method. The reducing sugars produced by α-amylase react with dinitro salicylic acid (DNS) and form a brown-coloured product, nitro amino salicylic acid. It was observed that Rotula aquatica-mediated AgNPs showed higher inhibition of α-amylase (Figure 10), ranging from 28.5% to 73.2% (at 50 to 250 µg/mL), compared to the standard, which ranged from 24.6% to 66.1% (at 50 to 250 µg/mL) (Table 8).

Table 8: Alpha amylase inhibition by *Rotula aquatica* mediated silver nanoparticle against the standard.

Concentration(µg/mL)	Metformin (%inhibition)	RQR-AgNP (% inhibition)
50	24. 6	28.5
100	39.7	45.8
150	49.5	56.7
200	58.4	65.9
250	66.1	73.2

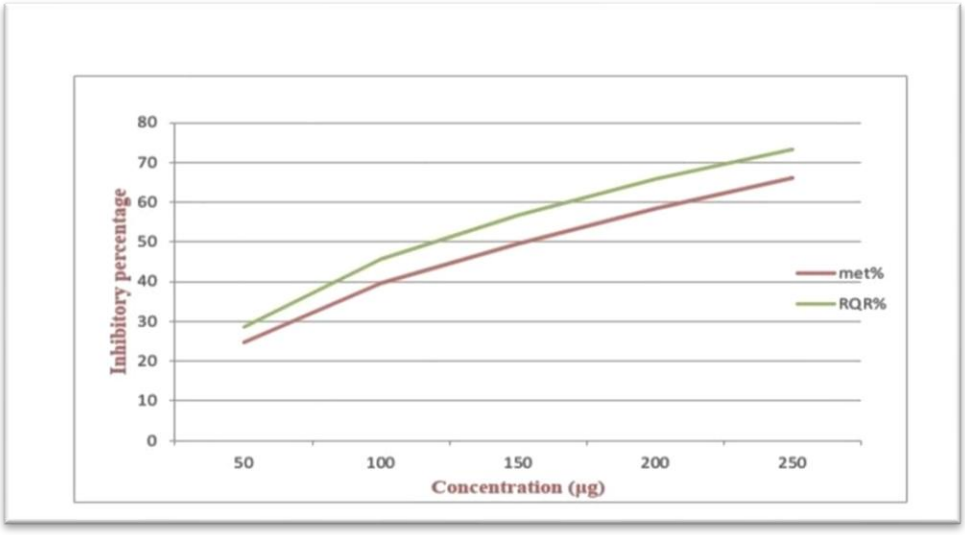


Figure 10: Alpha amylase inhibition by *Rotula aquatica* mediated silver nanoparticle

5.4.2 Glucose uptake assay

5.4.2.1 Standard curve

The standard calibration data showed a proportional increase in mean optical density (OD) with increasing 2-DG6P concentration (0–100 pmol), indicating a strong linear relationship between analyte concentration and absorbance (Table 9). This excellent linearity confirms the accuracy and reliability of the standard curve for the quantitative estimation of glucose uptake in the assay.

Table 9: OD reading of 2-DG6P standards

2-DG6P (pmol)	Mean OD
0	0.043
20	0.385
40	0.72
60	1.06
80	1.403
100	1.754

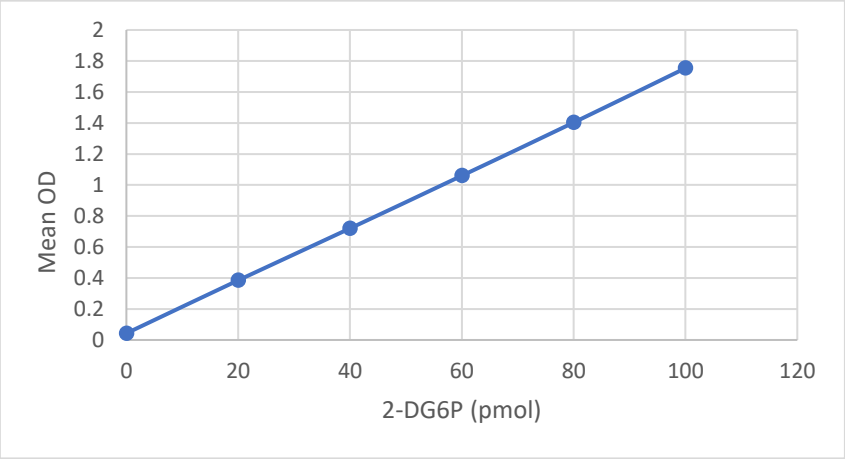


Figure 11: 2-DG6P standard curve obtained

The standard calibration curve demonstrated excellent linearity, with a coefficient of determination ($R^2 = 0.9999$) (Figure 11). The coefficient of determination was calculated using the equation $R^2 = 1 - (SSres/SStot)$, where SSres represents the residual sum of squares and SStot represents the total sum of squares. The high R^2 value indicates that 99.99% of the variation in absorbance is explained by the concentration of 2-deoxyglucose-6-phosphate (2-

DG6P), thereby validating the assay as highly reliable for the accurate quantification of glucose uptake.

5.4.2.2 *Rotula aquatica* - Effect on Glucose Uptake

The results demonstrated a concentration-dependent increase in glucose uptake following treatment with *Rotula aquatica* extract, with final 2-DG uptake increasing from 0.42 µM at 10 µg/mL to 0.83 µM at 100 µg/mL (Table 10). The marked increase at lower to intermediate concentrations, followed by a slight increase between 75 and 100 µg/mL, suggests that glucose uptake may approach saturation at higher extract concentrations.

Table 10: Concentration-dependent effect of *Rotula aquatica* extract on 2-DG uptake

Concentration of RQR (µg/mL)	Final 2-DG Uptake (µM)
10	0.42
25	0.57
50	0.73
75	0.81
100	0.83

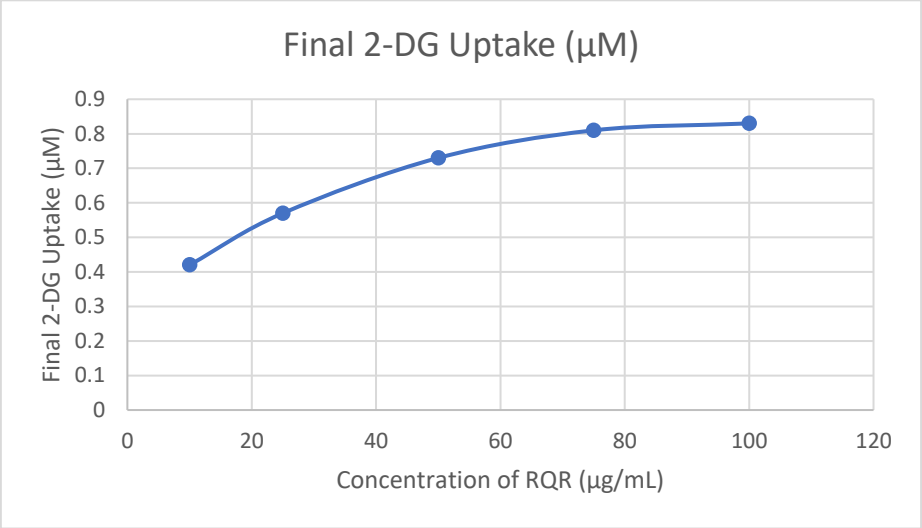


Figure 12: Dose response curve showing stimulation of 2-DG uptake by *Rotula aquatica* extract

The glucose uptake assay demonstrated that *Rotula aquatica* root extract significantly enhanced glucose uptake in a concentration-dependent manner, indicating its potential antihyperglycemic activity. The standard calibration curve generated using 2-deoxyglucose-6-phosphate (2-DG6P) standards exhibited excellent linearity, with a coefficient of determination (R^2 = 0.9999) (Figure 12), validating the precision and reliability of the assay for the quantitative estimation of glucose uptake. The final intracellular 2-DG uptake increased progressively from 0.42 µM at 10 µg/mL to 0.83 µM at 100 µg/mL, demonstrating that increasing concentrations of the extract promoted enhanced cellular glucose uptake. A marked

increase in glucose uptake was observed between 10 and 75 µg/mL, whereas only a marginal increase occurred between 75 and 100 µg/mL, suggesting that the glucose transport system may have approached saturation at higher extract concentrations. These findings indicate that *Rotula aquatica* root extract effectively stimulates cellular glucose utilization, possibly through the enhancement of glucose transporter activity or insulin-responsive signalling pathways. Overall, the results highlight *Rotula aquatica* as a promising natural therapeutic candidate for the management of diabetes mellitus and warrant further mechanistic studies and in vivo investigations to elucidate its mode of action and therapeutic efficacy.

5.5 Quantitative Real-Time PCR to assess the Relative Quantification

5.5.1 Total RNA isolation and cDNA preparation

Agarose gel electrophoresis of total RNA isolated from L6 cells treated with *Rotula aquatica* silver nanoparticles (RQR-AgNPs) and untreated control cells revealed two distinct ribosomal RNA bands corresponding to 28S rRNA and 18S rRNA(Figure 13). Both the treated and control samples exhibited sharp, well-defined bands without noticeable smearing, indicating that the isolated RNA was intact and of high quality.

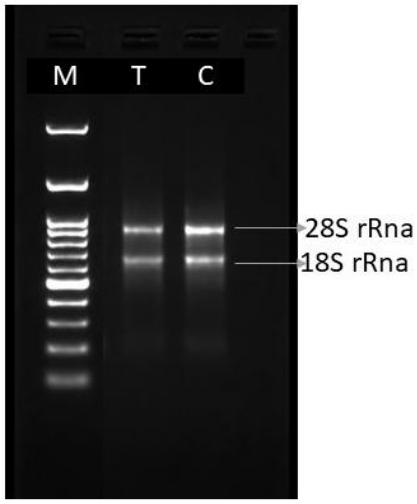


Figure 13: Agarose gel electrophoresis of total RNA isolated; T: L6 cells treated with *Rotula aquatica* silver nanoparticles (RQR-AgNPs) and C; untreated control cells revealed two distinct ribosomal RNA bands corresponding to 28S rRNA and 18S rRNA

These results confirmed that the RNA samples were suitable for subsequent cDNA synthesis and quantitative real-time PCR (qRT-PCR) analysis.

Complementary DNA (cDNA) was successfully synthesized from total RNA isolated from both the RQR-AgNP-treated and untreated control L6 cells. The quality of the synthesized cDNA and the efficiency of the primers were evaluated by quantitative real-time PCR (qRT-

PCR) using GAPDH as the reference gene. The amplification profile showed a characteristic sigmoidal curve with a Ct value of 19.09, indicating successful cDNA synthesis and sufficient template for downstream gene expression analysis.

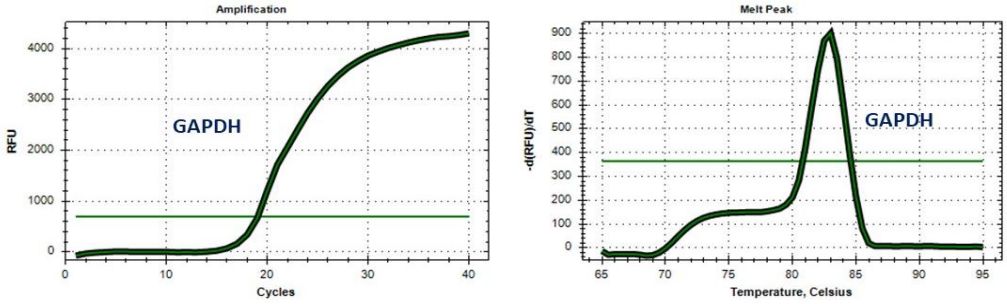


Figure 14: Representative qRT-PCR amplification and melt curve analysis of the GAPDH reference gene used for cDNA quality assessment

Melt curve analysis revealed a single, sharp peak for GAPDH amplification in both samples(Figure 14), confirming specific amplification, efficient primer performance, and the suitability of the synthesized cDNA for subsequent gene expression analysis.

5.5.2 Relative Quantification of GLUT 4 Gene Expression in Treated and Untreated L6 Cells

Based on the glucose uptake assay, 100 µg/mL was identified as the optimum concentration, as it produced the highest glucose uptake in L6 cells. Therefore, L6 cells were treated with 100 µg/mL of Rotula aquatica root extract-mediated silver nanoparticles (RQR-AgNPs) for 24 hours, and the relative expression of the GLUT 4 gene was quantified by qRT-PCR and compared with that of the untreated control cells.

The relative expression of the GLUT 4 gene in L6 cells treated with 100 µg/mL of Rotula aquatica root extract-mediated silver nanoparticles (RQR-AgNPs) was quantified by qRT-PCR using the 2^−ΔΔCt method, with GAPDH as the internal reference gene. As shown in the graph, the untreated control cells exhibited a normalized fold change of 1.0, whereas the treated cells showed a 1.31-fold increase in GLUT 4 gene expression. This result indicates that treatment with RQR-AgNPs upregulated GLUT 4 expression compared with the untreated control, suggesting enhanced glucose transport potential in skeletal muscle cells.

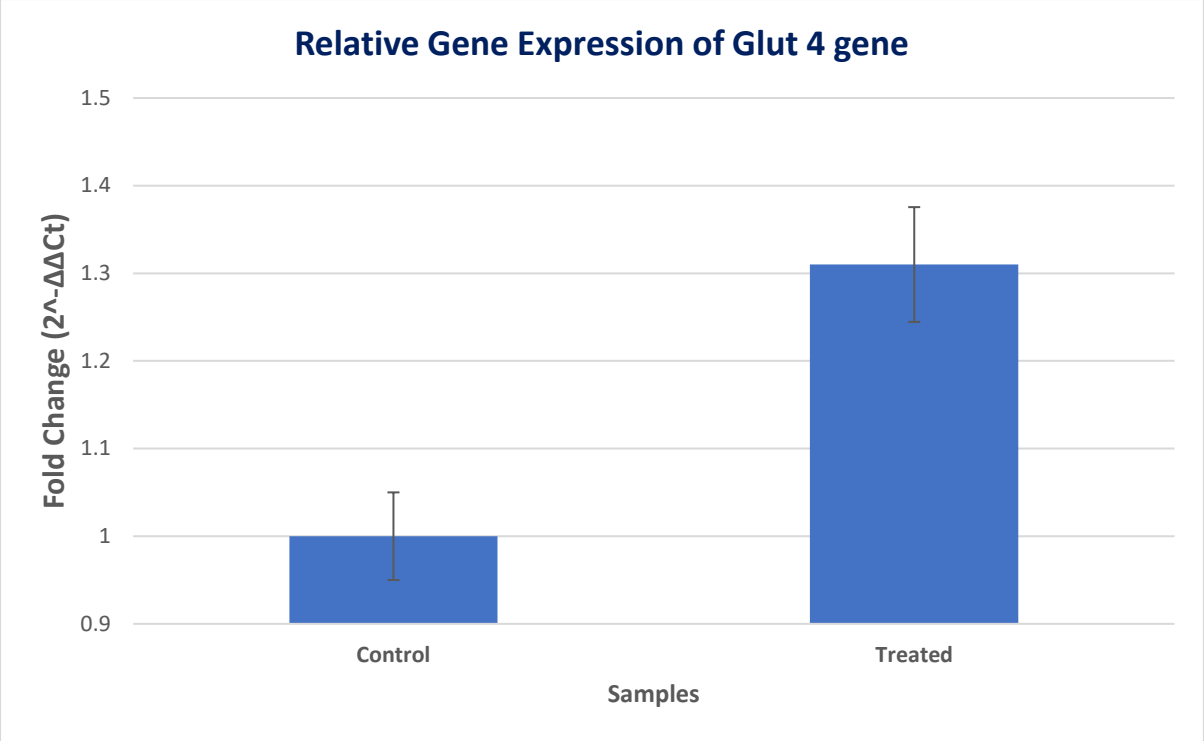


Figure 15: Relative expression of Glut 4 gene in treated and control samples determined by qRT-PCR; Relative expression values were calculated using the 2^-ΔΔCt method, with GAPDH as the internal reference

GLUT 4 is the principal insulin-responsive glucose transporter responsible for facilitating glucose uptake into skeletal muscle and adipose tissue. Increased GLUT 4 expression is associated with improved cellular glucose uptake and insulin sensitivity. The observed upregulation of GLUT4 is consistent with the glucose uptake assay, which showed enhanced 2-deoxyglucose uptake following treatment with RQR-AgNPs (Figure 15). These findings suggest that the antihyperglycemic activity of Rotula aquatica silver nanoparticles may be mediated, at least in part, by upregulation of GLUT4 expression, although further studies are required to confirm the underlying molecular mechanisms.

Chapter-6

Discussion

Diabetes mellitus is a chronic metabolic disorder characterized by persistent hyperglycemia resulting from impaired insulin secretion, impaired insulin action, or both. The rapidly increasing global prevalence of diabetes has accelerated the search for alternative therapeutic strategies, including plant-based nanomedicine. Green synthesis of nanoparticles using medicinal plants has attracted considerable attention due to its eco-friendliness, cost-effectiveness, and biocompatibility. Plant-derived phytochemicals, including phenolics, flavonoids, proteins, and other secondary metabolites, function as reducing, stabilizing, and capping agents during nanoparticle synthesis, thereby enhancing nanoparticle stability and biological activity.

The present study effectively synthesized silver nanoparticles (AgNPs) using *Rotula aquatica* root extract and evaluated their physicochemical characteristics and antidiabetic potential. The synthesized nanoparticles were characterized using UV–Visible spectroscopy, Dynamic Light Scattering (DLS), Fourier Transform Infrared (FTIR) spectroscopy, MTT cytotoxicity assay, α-amylase inhibition assay, glucose uptake assay, and qRT-PCR analysis. The formation of *Rotula aquatica*-mediated silver nanoparticles was confirmed by UV–Visible spectroscopy. A characteristic surface plasmon resonance (SPR) peak was observed at 447 nm, indicating the reduction of silver ions (Ag^{+}) into metallic silver nanoparticles (Ag^{0}). The SPR band arises from the collective oscillation of conduction electrons at the nanoparticle surface. Similar SPR absorption peaks in the 400–500 nm range have been reported for plant-mediated silver nanoparticles, depending on particle size, shape, and surface chemistry (Ahmed et al., 2016). Therefore, the observed absorption peak at 447 nm confirms the successful synthesis and stability of the synthesized AgNPs.

Dynamic Light Scattering (DLS) analysis demonstrated that the synthesized AgNPs possessed a narrow particle size distribution with a hydrodynamic diameter of approximately 45–50 nm. The presence of a single sharp peak indicated the formation of uniformly dispersed nanoparticles, while the absence of additional peaks at larger particle sizes suggested minimal aggregation and good colloidal stability. Similar observations have been reported for green-synthesized silver nanoparticles, where a narrow particle size distribution reflects efficient stabilization and uniform nanoparticle formation (Ahmed et al., 2016; Iravani et al., 2014).

FTIR analysis further confirmed the participation of *R. aquatica* phytochemicals in nanoparticle synthesis. The presence of hydroxyl and carbonyl functional groups indicated that bioactive compounds present in the root extract were involved in both the reduction of silver ions and stabilization of the synthesized nanoparticles. These phytochemicals not only function as natural reducing and capping agents but may also contribute to the biological activities of the nanoparticles. Similar findings have been reported for other plant-mediated silver nanoparticle synthesis studies (Ahmed et al., 2016).

The cytotoxicity of the synthesized AgNPs was evaluated using the MTT assay in HepG2 (human liver cancer cell line) and L6 cell lines (rat skeletal muscle myoblast cell line). The nanoparticles exhibited a concentration dependent effect on cell viability, with higher cell survival observed at lower concentrations. Notably, the IC_{50} value was higher in L6 cells than in HepG2 cells, indicating lower toxicity towards skeletal muscle cells. This observation is particularly important because skeletal muscle is the primary tissue responsible for insulin-mediated glucose uptake and maintenance of glucose homeostasis. Similar concentration-dependent cytotoxic effects of silver nanoparticles have been reported previously, where toxicity is influenced by nanoparticle size, concentration, surface characteristics, and cellular uptake (Asha Rani et al., 2009; Gliga et al., 2014). The comparatively lower toxicity observed in L6 cells may be attributed to the phytochemical constituents of *R. aquatica*, which likely function as biocompatible surface stabilizing agents.

The α-amylase inhibition assay was performed to evaluate the carbohydrate-hydrolyzing enzyme inhibitory activity of the synthesized AgNPs. α-Amylase is a key digestive enzyme that hydrolyses starch into absorbable sugars, thereby contributing to postprandial blood glucose elevation. Consequently, inhibition of α-amylase represents an effective therapeutic strategy for controlling postprandial hyperglycaemia.

In the present study, *Rotula aquatica*-mediated AgNPs exhibited significant α-amylase inhibitory activity (73.2%), comparable to that of the standard antidiabetic drug metformin. The observed inhibitory effect may result from the synergistic interaction between silver nanoparticles and phytochemicals present in *R. aquatica*, particularly phenolic and flavonoid compounds. Similar studies have demonstrated that plant-derived polyphenols possess strong α-amylase inhibitory activity and contribute significantly to antidiabetic effects (Tundis et al., 2010).

The glucose uptake assay demonstrated that *Rotula aquatica*-mediated AgNPs enhanced cellular glucose uptake in a concentration-dependent manner. The intracellular uptake of 2-deoxyglucose increased from 0.42 µM at 10 µg/mL to 0.83 µM at 100 µg/mL, indicating enhanced glucose utilization by the treated cells. The standard calibration curve exhibited excellent linearity (R^2 = 0.9999), confirming the accuracy and reliability of the assay. The enhanced glucose uptake observed in this study may be attributed to the presence of bioactive phytochemicals such as polyphenols and flavonoids, which are known to improve insulin sensitivity, regulate carbohydrate metabolism, stimulate glucose transporter activity, and promote cellular glucose uptake. Similar findings were reported by Hanhineva et al. (2010), who demonstrated that dietary polyphenols regulate carbohydrate metabolism and improve glucose handling by modulating multiple cellular signaling pathways. In the present study, the progressive increase in glucose uptake with increasing nanoparticle concentration indicates a dose-dependent antihyperglycemic effect. The greater glucose uptake observed at higher concentrations suggests that the active phytoconstituents of *R. aquatica*, together with the synthesized silver nanoparticles, enhance glucose transport into skeletal muscle cells.

During adipocyte maturation, the transcriptional activity of key insulin-signalling genes, including *Peroxisome proliferator-activated receptor gamma* (*Pparγ*) and *Glucose transporter-4* (*Glut-4*), is upregulated to promote glucose and fatty acid uptake, processes that are essential for adipogenesis (Kim et al., 2012). GLUT-4 is the principal insulin-responsive glucose transporter in adipose tissue and skeletal muscle. Upon insulin stimulation, GLUT-4-containing intracellular vesicles translocate to the plasma membrane, thereby facilitating cellular glucose uptake (Reaven et al., 1988). In type 2 diabetes mellitus (T2DM), insulin resistance disrupts this process by reducing GLUT-4 expression and impairing its translocation to the plasma membrane, resulting in diminished glucose uptake in insulin-sensitive tissues (Xu et al., 2017). Consequently, reduced GLUT-4 expression and impaired insulin responsiveness are considered hallmark features of T2DM. Previous studies using differentiated human adipocytes and mature 3T3-L1 adipocytes have similarly reported decreased GLUT-4 mRNA and protein expression, accompanied by defective GLUT-4 translocation under insulin-resistant conditions (Derici et al., 2021).

In the present study, qRT-PCR analysis demonstrated that treatment of L6 skeletal muscle cells with *Rotula aquatica* root extract mediated silver nanoparticles (RQR-AgNPs) significantly upregulated *Glut-4* mRNA expression compared with untreated control cells. This enhanced transcription correlated well with the increased glucose uptake observed in treated cells,

suggesting improved insulin responsiveness. Given the pivotal role of GLUT-4 in insulin-mediated glucose transport and the well-established association between increased GLUT-4 expression and improved insulin sensitivity, these findings indicate that RQR-AgNPs possess promising insulin-sensitizing potential. The combined enhancement of glucose uptake, α-amylase inhibition, and *Glut-4* gene expression demonstrates the multifaceted antidiabetic activity of *R. aquatica*-mediated silver nanoparticles. Therefore, these nanoparticles represent a promising candidate for improving glucose homeostasis and alleviating insulin resistance associated with T2DM. Nevertheless, further investigations involving GLUT-4 protein expression, membrane translocation studies, additional insulin signalling molecules, and in vivo diabetic models are required to validate these findings and elucidate the precise molecular mechanisms underlying their antidiabetic effects.

Summary and Conclusion

The present study investigated the green synthesis, characterization, and antidiabetic potential of *Rotula aquatica* root extract-mediated silver nanoparticles (RQR-AgNPs). Successful synthesis of the nanoparticles was confirmed by UV–Visible spectroscopy, as evidenced by the characteristic surface plasmon resonance peak at 447 nm. Dynamic Light Scattering (DLS) analysis revealed a uniform particle size distribution with good colloidal stability, while FTIR analysis confirmed the involvement of plant-derived phytochemicals as reducing and stabilizing agents during nanoparticle synthesis.

The biological evaluation demonstrated that RQR-AgNPs exhibited concentration-dependent cytotoxicity with lower toxicity toward L6 skeletal muscle cells than HepG2 cells, indicating good cellular compatibility for antidiabetic applications. The nanoparticles also showed significant α-amylase inhibitory activity comparable to metformin, suggesting their ability to reduce postprandial glucose levels. Furthermore, glucose uptake assays demonstrated a concentration-dependent enhancement of cellular glucose utilization, indicating improved glucose transport.

At the molecular level, qRT-PCR analysis revealed significant upregulation of *Glut-4* mRNA expression in L6 skeletal muscle cells following treatment with RQR-AgNPs. The increased *Glut-4* expression correlated with enhanced glucose uptake, suggesting improved insulin responsiveness. Collectively, these findings demonstrate that *R. aquatica*-mediated silver nanoparticles possess promising physicochemical characteristics, good biocompatibility, and significant antidiabetic activity through multiple mechanisms, including α-amylase inhibition, enhanced glucose uptake, and modulation of insulin-responsive glucose transporter expression.

References

A., V., S., A., Kuriakose, J., Midhun, S. J., Jyothis, M., & Latha, M. S. (2018). Protective effect of Rotula aquatica Lour. against gentamicin-induced oxidative stress and nephrotoxicity in Wistar rats. Biomedicine & Pharmacotherapy, 106, 1188–1195.

Agrawal, P., Mruthunjaya, K., Goyal, K., Ahuja, D., & Gupta, K. M. (2021). Analgesic, anti-inflammatory and antipyretic activity of Rotula aquatica Lour. leaves. Research Journal of Pharmacy and Technology, 14(10), 5503–5507.

Ahmad, S., Munir, S., Zeb, N., Ullah, A., Khan, B., Ali, J., ... & Ali, S. (2019). Green nanotechnology: A review on green synthesis of silver nanoparticles—An eco-friendly approach. International Journal of Nanomedicine, 14, 5087–5107.

Ahmed, S., Ahmad, M., Swami, B. L., & Ikram, S. (2016). A review on plant extract-mediated synthesis of silver nanoparticles for biological applications. Journal of Advanced Research, 7, 17–28.

Ansar, A., & Ansil, P. N. (2025). Rotula aquatica: A versatile medicinal shrub with diverse therapeutic applications. In M. K. Sinha (Ed.), Ethnobotany and Biodiversity of Medicinal Plants (Vol. 2, pp. 99–116). Helmand Books.

Anand, K., Tiloke, C., Naidoo, P., & Chuturgoon, A. A. (2017). Phytonanotherapy for management of diabetes using green synthesis nanoparticles. Journal of Photochemistry and Photobiology B: Biology, 173, 626–639.

Anju, T. R., Parvathy, S., Veettil, M. V., Rosemary, J., Ansalna, T. H., Shahzabanu, M. M., & Devika, S. (2021). Green synthesis of silver nanoparticles from Aloe vera leaf extract and its antimicrobial activity. Materials Today: Proceedings, 43, 3956–3960.

Arora, S., Ojha, S. K., & Vohora, D. (2009). Characterisation of streptozotocin-induced diabetes mellitus in Swiss albino mice. Global Journal of Pharmacology, 3(2), 81–84.

AshaRani, P. V., Mun, G. L. K., Hande, M. P., & Valiyaveettil, S. (2009). Cytotoxicity and genotoxicity of silver nanoparticles in human cells. ACS Nano, 3(2), 279–290.

Ashwini, C. S., Pramod, H. J., Rai, A. K., Asnani, G. P., & Patil, M. B. (2012). Antidiabetic activity of Rotula aquatica roots in diabetic rats. Journal of Pharmaceutical and Scientific Innovation, 1(3), 14–17.

Asplund, K., Wiholm, B. E., & Lithner, F. (2008). Glibenclamide-associated hypoglycaemia: A report on 57 cases. Pakistan Journal of Pharmaceutical Sciences, 24, 6–16.

Aswathanarayan, J. B., & Vittal, R. R. (2013). In vitro evaluation of antioxidant and antibacterial activities of Rotula aquatica and Ancistrocladus heyneanus. Journal of Pharmacy Research, 6(2), 313–317.

Baby, B., Kopilakkal, R., Rani, S., Rasheed, P. S., & Azeem, A. K. (2017). Rotula aquatica Lour.: A review on medicinal uses, phytochemistry and pharmacological actions. Indian Journal of Pharmaceutical and Biological Research, 5(4), 4–9.

Balan, K., Qing, W., Wang, Y., Liu, X., Palvannan, T., Wang, Y., ... & Zhang, Y. (2016). Antidiabetic activity of silver nanoparticles from green synthesis using Lonicera japonica leaf extract. RSC Advances, 6(46), 40162–40168.

Basch, E., Gabardi, S., & Ulbricht, C. (2003). Bitter melon (Momordica charantia): A review of efficacy and safety. American Journal of Health-System Pharmacy, 60(4), 356–359.

Bastaki, S. (2005). Diabetes mellitus and its treatment: A review. International Journal of Diabetes & Metabolism, 13, 111–134.

Bency, B. T., Remya, K., Rani, S., Rasheed, P. S., & Azeem, A. K. (2017b). Rotula aquatica Lour.: A review on medicinal uses, phytochemistry and pharmacological actions. Indian Journal of Pharmaceutical and Biological Research, 5(4), 4–9.

Bhanu Priya, Gahlot, M., Joshi, P., Zade, S., & Bagmar, U. (2014). Evaluation of anti-diabetic activity of methanolic extract from the leaves of Rotula aquatica Lour. in alloxan-induced diabetic rats. Pharmacognosy Journal, 6(2).

Bhatia, S. K., Hadden, D. R., Montgomery, D. A. D., & Weaver, J. A. (1970). Glibenclamide therapy in diabetes mellitus. Journal of Diabetic Pharmacology and Physiology, 13, 23–32.

Blair, M. (2016). Diabetes mellitus review. Urology Nursing, 36(1), 27–36.

Castillo-Henríquez, L., Alfaro-Aguilar, K., Ugalde-Álvarez, J., Vega-Fernández, L., Montes de Oca-Vásquez, G., & Vega-Baudrit, J. R. (2020). Green synthesis of gold and silver nanoparticles from plant extracts and their possible applications as antimicrobial agents in the agricultural area. Nanomaterials, 10(9), 1763.

Chempakam, B. (1993). Hypoglycemic activity of arecoline in betel nut (Areca catechu L.). Indian Journal of Experimental Biology, 31, 474–475.

Cho, N. H., Shaw, J. E., Karuranga, S., Huang, Y., da Rocha Fernandes, J. D., Ohlrogge, A. W., & Malanda, B. (2018). IDF Diabetes Atlas: Global estimates of diabetes prevalence for 2017 and projections for 2045. Diabetes Research and Clinical Practice, 138, 271–281.

Christina, A. J. M., Priya Mole, M., & Moorthy, R. (2002). Studies on the antilithic effect of Rotula aquatica Lour. in male Wistar rats. Methods and Findings in Experimental and Clinical Pharmacology, 24(6), 357–359.

Cousin, E., Duncan, B. B., Stein, C., Ong, K. L., Vos, T., Yunusa, I., … & GBD 2019 Diabetes Mortality Collaborators. (2022). Diabetes mortality and trends before 25 years of age: An analysis of the Global Burden of Disease Study 2019. The Lancet Diabetes & Endocrinology, 10(3), 177–192. Doi.org

Derici GE, Özdaş S, Canatar İ, Koç M. Antidiabetic activities of Bolanthus spergulifolius (Caryophyllaceae) extracts on insulin-resistant 3T3-L1 adipocytes. PLoS One. 2021 Jun 16;16(6): e0252707. doi: 10.1371/journal.pone.0252707. PMID: 34133443; PMCID: PMC8208533.

Dewanjee, S., Dey, P., Chacko, M. J., & Dutta, R. (2020). Green synthesis of nanoparticles and their therapeutic applications. Trends in Biotechnology, 38(3), 243–254.

Diatewa, M., Samba, C. B., Assah, T. C., & Abena, A. A. (2004). Hypoglycemic and antihyperglycemic effects of the diethyl ether fraction isolated from the aqueous extract of the leaves of Cogniauxia podoleana Baillon in normal and alloxan-induced diabetic rats. Journal of Ethnopharmacology, 92, 229–232.

Dinparvar, S., Naderi-Meshkin, H., Mahdipour, E., Mafigholami, R., Sadri, B., & Sharifi, A. M. (2020). Current approaches in treatment of diabetic retinopathy and future prospects. Medical Journal of the Islamic Republic of Iran, 34, Article 63. Doi.org

Eddouks, M., Lemhadri, A., & Michel, J. B. (2004). Caraway and caper: Potential antihyperglycaemic plants in diabetic rats. Journal of Ethnopharmacology, 94, 143–148.

Eshrat, M. H. (2003). Effect of Coccinia indica (L.) and Abroma augusta (L.) on glycemia, lipid profile and on indicators of end-organ damage in streptozotocin induced diabetic rats. Indian Journal of Clinical Biochemistry, 18(2), 54-63.

Farwa, U., Khan, M. I., & Ali, S. (2022). Diabetes mellitus: Pathophysiology, diagnosis, and management. Journal of Diabetes & Metabolic Disorders, 21(1), 1–10.

Fitipaldi, H., McCarthy, M. I., Florez, J. C., & Franks, P. W. (2018). A global overview of precision medicine in type 2 diabetes. Diabetes, 67(10), 1911–1922.

Gadang, V., Gilbert, W., Hettiarachchy, N., Horax, R., Katwa, L., & Devareddy, L. (2011). Dietary bitter melon seed increases peroxisome proliferator-activated receptor-γ gene expression in adipose tissue, down-regulates nuclear factor-κB expression, and alleviates symptoms associated with metabolic syndrome. Journal of Medicinal Food, 14(1–2), 86–.

Galicia-Garcia, U., Benito-Vicente, A., Jebari, S., Larrea-Sebal, A., Siddiqi, H., Uribe, K. B., Ostolaza, H., & Martín, C. (2020). Pathophysiology of type 2 diabetes mellitus. International Journal of Molecular Sciences, 21(17), 6275.

Gliga, A. R., Skoglund, S., Odnevall Wallinder, I., Fadeel, B., & Karlsson, H. L. (2014). Size-dependent cytotoxicity of silver nanoparticles in human lung cells: The role of cellular uptake, agglomeration, and Ag release. Particle and Fibre Toxicology.

Gregg, E. W., Li, Y., Wang, J., Rios Burrows, N., Ali, M. K., Rolka, D., … & Geiss, L. (2014). Changes in diabetes-related complications in the United States, 1990–2010. New England Journal of Medicine, 370(16), 1514-1523.

Grover, J. K., & Yadav, S. P. (2004). Pharmacological actions and potential uses of Momordica charantia: A review. Journal of Ethnopharmacology, 93(1), 123–132.

Gupta, M. G., Mruthunjaya, K., Saini, L., Garg, S. K., Agrawal, S. G., & Goyal, S. (2011). Analgesic, anti-inflammatory and antipyretic activity of Rotula aquatica Lour. root. Inventi Rapid: Planta Activa, 3, 037.

Hanhineva, K., Torronen, R., Bondia-Pons, I., Pekkinen, J., Kolehmainen, M., Mykkänen, H., & Poutanen, K. (2010). Impact of dietary polyphenols on carbohydrate metabolism. International Journal of Molecular Sciences, 11(4), 1365–1402. https://doi.org/10.3390/ijms11041365

Hannan, J. M. A., Marenah, L., Ali, L., Rokeya, B., Flatt, P. R., & Abdel-Wahab, Y. H. A. (2006). Ocimum sanctum leaf extracts stimulate insulin secretion from perfused pancreas, isolated islets and clonal pancreatic β-cells. Journal of Endocrinology, 189(1), 127–136.

Haq, F. U., Siraj, A., Ameer, M. A., Hamid, T., Rahman, M., Khan, S., ... & Siraj, A. (2021). Comparative review of drugs used in diabetes mellitus: New and old. Journal of Diabetes Mellitus, 11(4), 115–131.

Hasan, M., Ahmed, S., & Islam, M. (2018). Plant-derived antidiabetic compounds: Safety and efficacy. BMC Complementary and Alternative Medicine, 18(1), 189.

Huq, M. A., Ashrafudoulla, M., Rahman, M. M., Balusamy, S. R., & Akter, S. (2022). Green synthesis and potential antibacterial applications of bioactive silver nanoparticles: A review. Polymers, 14(4), 742.

Hussain, I., Singh, N. B., Singh, A., Singh, H., & Singh, S. C. (2016). Green synthesis of nanoparticles and its potential application. Biotechnology Letters, 38(4), 545–560.

Iravani, S., Korbekandi, H., Mirmohammadi, S. V., & Zolfaghari, B. (2014). Synthesis of silver nanoparticles: Chemical, physical and biological methods. Research in Pharmaceutical Sciences, 9(6), 385–406.

Ismail, M. Y. (2009). Clinical evaluation of antidiabetic activity of Trigonella seeds and Aegle marmelos leaves. World Applied Sciences Journal, 7(10), 1231–1234.

Jacob, B., & Narendhirakannan, R. T. (2019). Role of medicinal plants in the management of diabetes mellitus: A review. 3 Biotech, 9(1), 4.

Jarald, E. E., Joshi, S. B., & Jain, D. C. (2008). Antidiabetic activity of aqueous extract and non-polysaccharide fraction of Cynodon dactylon Pers. Indian Journal of Experimental Biology, 46, 660–667.

Jijith, U. S., & Jayakumari, S. (2017). Recent advances and methods for in-vitro evaluation of antidiaetic activity: A review. International Journal of Research in Ayurveda & Pharmacy, 8(1), 81-87.

Joshi, S. R., & Parikh, R. M. (2007). India—Diabetes capital of the world: Now heading towards hypertension. Journal of the Association of Physicians of India, 55, 323–324.

Jothivel, N., Ponnusamy, S. P., Appachi, M., & Panneerselvam, A. (2007). Antidiabetic activities of methanol leaf extract of Costus pictus D. Don in alloxan-induced diabetic rats. Journal of Health Science, 53(6), 655–663.

Kamurthy, H., Nampally, S., & Dontha, S. (2014). Anti-inflammatory activity of Rotula aquatica Lour. in albino rats. International Journal of Pharmaceutical Sciences and Drug Research, 48–51.

Khan, V., Najmi, A. K., Akhtar, M., Aqil, M., Mujeeb, M., & Pillai, K. K. (2012). A pharmacological appraisal of medicinal plants with antidiabetic potential. Journal of Pharmacy and Bioallied Sciences, 4(1), 27–42.

Khattak, A., Ahmad, B., Rauf, A., Bawazeer, S., Farooq, U., Ali, J., ... & Linfang, H. (2019). Green synthesis, characterisation and biological evaluation of plant-based silver nanoparticles using Quercus semecarpifolia Smith aqueous leaf extract. IET Nanobiotechnology, 13(1), 36–42.

Kim GS, Park HJ, Woo JH, Kim MK, Koh PO, Min W, et al. Citrus aurantium flavonoids inhibit adipogenesis through the Akt signaling pathway in 3T3-L1 cells. BMC Compl Alternative Med. 2012;12(1):31. doi: 10.1186/1472-6882-12-31

Krawinkel, M. B., & Keding, G. B. (2006). Bitter gourd (Momordica charantia): A dietary approach to hyperglycaemia. Nutrition Reviews, 64(7), 331–337.

Kuroda, M., Mimaki, Y., Nishiyama, T., Mae, T., Kishida, H., Tsukagawa, M., Takahashi, K., Kawada, T., Nakagawa, K., & Kitahara, M. (2005). Hypoglycemic effects of turmeric (Curcuma longa L. rhizomes) on genetically diabetic KK-Ay mice. Biological & Pharmaceutical Bulletin, 28, 937–939.

Lakshmi, K. V., Triveni, K. B., Anitha, S., & Shashidhara, S. (2012). In vitro anthelmintic activity of Rotula aquatica Lour. bark. Pharma Science Monitor, 3(4), 2332–2339.

Leung, L., Birtwhistle, R., Kotecha, J., Hannah, S., & Cuthbertson, S. (2009). Anti-diabetic and hypoglycaemic effects of Momordica charantia (bitter melon): A mini review. British Journal of Nutrition, 102(12), 1703–1708.

Livak, K. J., & Schmittgen, T. D. (2001). Analysis of relative gene expression data using real time quantitative PCR and the 2− ΔΔCT method. methods, 25(4), 402-408.

Mamedov, N., Craker, L. E., & Gardner, Z. (2012). Medicinal plants and their role in human life. Journal of Medicinal Food, 15(10), 913–920.

Mechchate, H., Es-Safi, I., Louba, A., Alqahtani, A. S., Nasr, F. A., Noman, O. M., ... & Bousta, D. (2021). In vitro alpha-amylase and alpha-glucosidase inhibitory activity and in vivo antidiabetic activity of Withania frutescens L. foliar extract. Molecules, 26(2), 293.

Medici, S., Peana, M., Nurchi, V. M., & Zoroddu, M. A. (2019). Medical uses of silver: History, myths, and scientific evidence. Journal of Medicinal Chemistry, 62(13), 5923–5943.

Mengi, A. S., & Bakshi, V. J. (2009). Evaluation of the aqueous extract of Rotula aquatica roots in acute and chronic inflammatory conditions in rats. Pharmaceutical Biology, 47(6), 491–495.

Nair, R., Kalariya, T., & Chanda, S. (2005). Antibacterial activity of some selected Indian medicinal flora. Turkish Journal of Biology, 29, 41–47.

Narayanan, E. S., Abdelgawad, A. M., Althobaiti, S. Y., Ghoneim, M. M., Rajamma, G. R., Sekhar, N., Parambi, T. G. D., Nath, R. L., Kanthlal, S. K., & Mathew, B. (2022). Effect of hydroalcoholic extract of Rotula aquatica Lour. on gentamicin-induced nephrotoxicity in Wistar albino rats: An in vitro and in vivo approach. Journal of Biomedical Nanotechnology, 18(3), 884–890.

Narendhirakannan, R. T., Subramanian, S., & Kandaswamy, M. (2006). Biochemical evaluation of antidiabetogenic properties of some commonly used Indian plants on streptozotocin-induced diabetes in experimental rats. Clinical and Experimental Pharmacology and Physiology, 33(12), 1150–1157.

Pallavi, M., Ramesh, K. C., Krishna, V., Channakeshava, H. G., & Jamuna, K. S. (2016). Total phenolics and antioxidant potential of Rotula aquatica Lour. Journal of Applied Pharmaceutical Science, 6(4), 169–174.

Pari, L., & Satheesh, M. A. (2004). Antidiabetic activity of Boerhaavia diffusa L.: effect on hepatic key enzymes in experimental diabetes. Journal of ethnopharmacology, 91(1), 109-113.

Patel, D. K., Prasad, S. K., Kumar, R., & Hemalatha, S. (2012). An overview on antidiabetic medicinal plants having insulin-mimetic property. Asian Pacific Journal of Tropical Biomedicine, 2(4), 320–330.

Patil, S., Narayanan, S., Eibl, G., & Jolly, I. C. (2004). Evaluation of antimitotic activity of Rotula aquatica (Lour.): A traditional herb used in the treatment of cancer. Indian Journal of Experimental Biology, 42(9), 893–899.

Pattanayak, P., Behera, P., Das, D., & Panda, S. (2010). Ocimum sanctum Linn.: A reservoir plant for therapeutic applications—An overview. Pharmacognosy Reviews, 4(7), 95–105.

Perumalsamy, R., & Krishnadhas, L. (2022). Anti-diabetic activity of silver nanoparticles synthesized from the hydroethanolic extract of Myristica fragrans seeds. Applied Biochemistry and Biotechnology, 194(3), 1136–1148.

Priya, B., Zade, S., Shaikh, A., Gahlot, M., & Joshi, P. (2013). In vitro antioxidant activity and determination of total phenolic and flavonoid contents of stems of Rotula aquatica Lour. International Journal of Pharmaceutical Sciences and Research, 4(9), 3608–3613.

Ramachandran, A., Das, A. K., & Joshi, S. R. (2010). Current status of diabetes in India and need for novel therapeutic agents. Supplement to Journal of the Association of Physicians of India, 58, 7–9.

Rameshwar, Y. H., Vijayakumari, B., Sasikala, V., & Radha, R. S. (2016). HPTLC fingerprinting of aqueous root extract of Rotula aquatica for phenol, tannin and saponin contents. Der Pharmacia Lettre, 8(8), 339–346.

Rana, A., Yadav, K., & Jagadevan, S. (2020). A comprehensive review on green synthesis of nature-inspired metal nanoparticles: Mechanism, application and toxicity. Journal of Cleaner Production, 272, 122880.

Raut, A. A., Sunder, S., Sarkar, S., Pandita, N. S., & Vaidya, A. D. B. (2008). Preliminary study on crystal dissolution activity of Rotula aquatica, Commiphora wightii, and Boerhaavia diffusa extracts. Fitoterapia, 79(7–8), 544–547.

Reaven GM. Banting lecture 1988. Role of insulin resistance in human disease. Diabetes. 1988;37(12):1595–607. doi: 10.2337/diab.37.12.1595

Rehman, H., Ali, W., Ali, M., Khan, N. Z., Aasim, M., Khan, A. A., ... & Hashmi, S. S. (2023). Delphinium uncinatum-mediated green synthesis of AgNPs and its antioxidant, enzyme inhibitory, cytotoxic, and antimicrobial potentials. PLoS ONE, 18(4), e0280553.

Restrepo, C. V., & Villa, C. C. (2021). Synthesis of silver nanoparticles: Influence of capping agents and dependence on size and shape. Environmental Nanotechnology, Monitoring & Management, 15, 100428.

Saleem, R., Ahmad, M., Hussain, S. A., Qazi, A. M., Ahmad, S. I., Qazi, M. H., Ali, M., Faizi, S., Akhtar, S., & Husnain, S. N. (1999). Hypotensive, hypoglycemic and toxicological studies on the flavonol C-glycoside shamimin from Bombax ceiba. Planta Medica, 65, 331–334.

Sarkhail, P., Rahmanipour, S., Fadyevatan, S., Mohammadirad, A., Dehghan, G., Amin, G., … & Abdollahi, M. (2007). Antidiabetic effect of Phlomis anisodonta: effects on hepatic cells lipid peroxidation and antioxidant enzymes in experimental diabetes. Pharmacological Research, 56(3), 261-266.

Sasikala, V., Radha, S. R., & Vijayakumari, B. (2013). In vitro evaluation of Rotula aquatica Lour. for antiurolithiatic activity. Journal of Pharmacy Research, 6(3), 378–382.

Shih, C. C., Lin, C. H., Lin, W. L., & Wu, J. B. (2009). Momordica charantia extract on insulin resistance and the skeletal muscle GLUT4 protein in fructose-fed rats. Journal of Ethnopharmacology, 123(1), 82-90.

Shyam, T., & Ganapaty, S. (2013). Phytochemical and biological studies of Rotula aquatica Lour. roots. Indian Drugs, 50(11), 34–38.

Shyam, T., Ganapaty, S., & Balakrishnaiah, P. (2013). Antidiabetic activity of Rotula aquatica Lour. roots in streptozotocin-induced diabetic rats. American Journal of Phytomedicine and Clinical Therapeutics, 1(7), 530–535.

Simmonds, M., Howes, M. J. R., & Soumyanath, A. (2006). Plants used in the treatment of diabetes. In Traditional Medicines for Modern Time: Antidiabetic Plants (6th ed., pp. 19–82). CRC Press/Taylor & Francis.

Singh, D., Singh, B., & Goel, R. K. (2011). Traditional uses, phytochemistry and pharmacology of Ficus religiosa: A review. Journal of Ethnopharmacology, 134(3), 565–583.

Singh, S., Rai, A. K., Sharma, P., Barshiliya, Y., Sihare, M., & Negi, A. (2012). Antidiarrhoeal activity of Rotula aquatica in rats. Asian Pacific Journal of Tropical Biomedicine, 2(1, Suppl.), S175–S177.

Sivakumar, T. (2021). A modern review of silver nanoparticles mediated by plant extracts and their potential bioapplications. International Journal of Botany Studies, 6(3), 170–175.

Sivaprasad, S., Gupta, B., Crosby-Nwaobi, R., & Evans, J. (2012). Prevalence of diabetic retinopathy in various ethnic groups in the world: A review. Survey of Ophthalmology, 57(4), 347–370.

Somani, R., Kasture, S., & Singhai, A. K. (2006). Antidiabetic potential of Butea monosperma in rats. Fitoterapia, 77, 86–90.

Subramoniam, A., Pushpangadan, P., Rajasekharan, S., Evans, D. A., Latha, P. G., & Valsaraj, R. (1996). Effects of Artemisia pallens Wall. on blood glucose levels in normal and alloxan-induced diabetic rats. Journal of Ethnopharmacology, 50, 13–17.

Tsai, C., Chen, E. C., Tsay, H., & Huang, C. (2012). Wild bitter gourd improves metabolic syndrome: A preliminary dietary supplementation trial. Nutrition Journal, 11(1), Article 4.

Tundis, R., Loizzo, M. R., & Menichini, F. (2010). Natural products as α-amylase and α-glucosidase inhibitors and their hypoglycaemic potential in the treatment of diabetes: An update. Mini-Reviews in Medicinal Chemistry, 10(4), 315–331.

Venkatachalam, S., Radha, R. S., & Vijayakumari, B. (2013). In vitro evaluation of Rotula aquatica Lour. for antiurolithiatic activity. Journal of Pharmacy Research, 6(3), 378–382.

Vijayakumari, B., Sumithra, S., Sasikala, V., & Radha, S. R. (2013). Evaluation of enzymatic and non-enzymatic antioxidant potential of Rotula aquatica Lour. Journal of Pharmacy Research, 6(5), 442.

Vijayvargia, R., Kumar, M., & Gupta, S. (2000). Hypoglycemic effect of aqueous extract of Enicostemma littorale Blume (chhotachirayata) on alloxan-induced diabetes mellitus in rats. Indian Journal of Experimental Biology, 38, 781–784.

Vysakh, A., Jayesh, K., Helen, L. R., Jyothis, M., & Latha, M. S. (2020). Acute oral toxicity and anti-inflammatory evaluation of methanolic extract of Rotula aquatica roots in Wistar rats. Journal of Ayurveda and Integrative Medicine, 11(1), 45–52.

Vysakh, A., Jayesh, K., Jisha, N., Vijeesh, V., Midhun, S. J., Jyothis, M., & Latha, M. S. (2022). Rotula aquatica Lour. mitigates oxidative stress and inflammation in acute pyelonephritic rats. Archives of Physiology and Biochemistry, 128(1), 92–100.

Vysakh, A., Raji, R. N., Latha, M. S., & Jyothis, M. (2016). Traditional and therapeutic importance of Rotula aquatica Lour.: An overview. International Journal of Pharmaceutical and Phytopharmacological Research, 7(3), 97–107.

Welihinda, J., Arvidson, G., Gylfe, E., Hellman, B., & Karlsson, E. (1982). The insulin-releasing activity of the tropical plant _Momordica charantia_. _Acta Biologica et Medica Germanica, 41(12), 1229–1240. 42a8

Whiting, D. R., Guariguata, L., Weil, C., & Shaw, J. (2011). IDF Diabetes Atlas: Global estimates of the prevalence of diabetes for 2011 and 2030. Diabetes Research and Clinical Practice, 94(3), 311–321.

Wild, S., Roglic, G., Green, A., Sicree, R., & King, H. (2004). Global prevalence of diabetes: Estimates for the year 2000 and projections for 2030. Diabetes Care, 27(5), 1047–1053.

Xu F, Gu D, Wang M, Zhu L, Chu T, Cui Y, et al. Screening of the potential α-amylase inhibitor in essential oil from Cedrus deodara cones. Ind Crops Prod. 2017:103:251–256. doi: 10.1016/j.indcrop.2017.04.006

Yazdanparast, R., Ardestani, A., & Jamshidi, S. (2007). Experimental diabetes treated with Achillea santolina: Effect on pancreatic oxidative parameters. Journal of Ethnopharmacology, 112, 13–18.

Yoshikawa M., Murakami, T., Kadoya, M., Matsuda, H., Muraoka, O., Yamahara J., & Murakami, N. (1996). Medicinal foodstuffs. III. Sugar beet (1): Hypoglycemic oleanolic acid oligoglycosides, betavulgarosides, I, II, III, and IV, from the root of Beta vulgaris L. (Chenopodiaceae). Chemical and pharmaceutical bulletin, 44(6), 1212-1217.

Youn, J. Y., Park, H. Y., & Cho, K. H. (2004). Anti-hyperglycemic activity of Commelina communis L.: Inhibition of α-glucosidase. Diabetes Research and Clinical Practice, 66(Suppl. 1), S149–S155.